
Towards Alternative Techniques for Improving Adversarial Robustness: Analysis of Adversarial Training at a Spectrum of Perturbations

Kaustubh Sridhar¹ Souradeep Dutta¹ Ramneet Kaur¹ James Weimer¹ Oleg Sokolsky¹ Insup Lee¹

Abstract

Adversarial training (AT) and its variants have spearheaded progress in improving neural network robustness to adversarial perturbations and common corruptions in the last few years. Algorithm design of AT and its variants are focused on training models at a specified perturbation strength ϵ and only using the feedback from the performance of that ϵ -robust model to improve the algorithm. In this work, we focus on models, trained on a spectrum of ϵ values. We analyze three perspectives: model performance, intermediate feature precision and convolution filter sensitivity. In each, we identify alternative improvements to AT that otherwise wouldn't have been apparent at a single ϵ . Specifically, we find that for a PGD attack at some strength δ , there is an AT model at some slightly larger strength ϵ , but no greater, that generalizes best to it. Hence, we propose overdesigning for robustness where we suggest training models at an ϵ just above δ . Second, we observe (across various ϵ values) that robustness is highly sensitive to the precision of intermediate features and particularly those after the first and second layer. Thus, we propose adding a simple quantization to defenses that improves accuracy on seen and unseen adaptive attacks. Third, we analyze convolution filters of each layer of models at increasing ϵ and notice that those of the first and second layer may be solely responsible for amplifying input perturbations. We present our findings and demonstrate our techniques through experiments with ResNet and WideResNet models on the CIFAR-10 and CIFAR-10-C datasets.¹

1. Introduction

Adversarial training (AT) is currently the most effective method to improve the adversarial robustness of neural networks. AT and its variants have created robust models with state-of-the-art results against white-box attacks (Croce et al., 2020) without having to resort to obfuscated gradients (Athalye et al., 2018). Various studies on the effects of hyperparameters (Pang et al., 2020; Sridhar et al., 2021; Goyal et al., 2020; Xie & Yuille, 2019), data augmentation (Rebuffi et al., 2021), unlabelled data (Carmon et al., 2019; Goyal et al., 2021; Sehwag et al., 2021), model size (Huang et al., 2021; Wu et al., 2021) and performance on unseen attacks (Stutz et al., 2020; Laidlaw et al., 2020) on AT have been conducted in the past.

But each study has been restricted to analysis at a specified defense perturbation strength ϵ (usually 8/255 for L_∞ adversarial robustness). For a fixed ϵ -robust model, each of the studies above suggests an algorithm in addition to a combination of hyperparameters to improve robustness. By not observing the variation across ϵ values, current methods miss out on potential ideas that can aid robustness. In this work, we present three such ideas. These ideas employ feedback from three different sources.

First, based on the performance of models adversarially trained at various ϵ 's, we find that there exists a defense perturbation strength ϵ (higher than the attack perturbation strength δ) at which an AT model generalizes best to an attack. All models trained with strengths greater or lesser than this value are less effective defenses. We suggest *overdesigning*, where for a given δ , a defender must train models at increasing $\epsilon > \delta$ until the validation error starts deteriorating. The recommendation would be to use the last model before degradation sets off, as the overdesigned defense (Section 3). In contrast, to the above adversarial robustness case are the more natural corruptions. Quite unexpectedly, we observe that lower ϵ 's create better models for classifying images with common corruptions (Section 6) & diagnose this issue as an effect of Pre-ReLU features.

Second, we notice that the precision of intermediate features strongly influences robustness. We show that simple *quantization* (especially after the first or second layer) in-

¹PRECISE Center, University of Pennsylvania. Correspondence to: Kaustubh Sridhar <ksridhar@seas.upenn.edu>.

¹Code: https://github.com/perturb-spectrum/analysis_and_methods

creases robustness of models trained at various ϵ 's to seen & unseen adaptive attacks. This observation as well, is not obvious at a unit value of ϵ , but can be seen to vary across the spectrum, for different values (Section 4).

Third, we show that the first and second layers' convolution filters are increasingly responsible for amplifying input perturbations in ResNet and WideResNet models for increasing ϵ (Section 5).

We demonstrate the above findings and the associated alternative techniques using ResNet18 and WideResNet-28-10 (with Swish activation functions) (Gowal et al., 2020) models on the CIFAR-10 and CIFAR-10-C (Hendrycks & Ditterich, 2019) datasets. Our contributions are summarized below:

- To the best of our knowledge, our work is the first to leverage information from adversarial trained ϵ -robust models at increasing levels of ϵ . Based on our observations, we suggest techniques to improve AT that is hard to fathom from a traditional analysis at one ϵ .
- We propose an *overdesigning* strategy that can consistently promise increased robustness to adversarial perturbations and demonstrate it with ResNet and WideResNet models on the CIFAR-10 dataset.
- We propose *quantization* of intermediate features that improves robustness for ResNet and WideResNet models on seen and unseen adaptive attacks (BPDA (Athalye et al., 2018) and Transfer PGD (Croce et al., 2022)) on the CIFAR-10 dataset.
- We perform a study of convolution filters at increasing ϵ and identify the first and second layers of ResNet and WideResNet models, as sole suspects for input perturbation propagation.

2. Background

2.1. Adversarial Training

Projected Gradient Descent based Adversarial training (PGD-AT) (Madry et al., 2018) solves a min-max optimization problem on a loss function l as

$$\min_{\theta} \mathbb{E}_{(x,y) \sim \mathcal{D}} \left[\max_{x' \in \mathcal{S}(x)} l(f_{\theta}(x'), y) \right]. \quad (1)$$

Above, \mathcal{D} represents the distribution over training data and $\mathcal{S}(x)$ is the allowed set of perturbed examples around x , usually in an L_p norm-bounded ball given by $\mathcal{S}(x) = \{x' \mid \|x' - x\|_p \leq \kappa\}$ where κ is the perturbation strength. The inner maximization, which obtains the adversarial example, takes place with the projected gradient descent (PGD) attack and uses a step size α

$$x^{i+1} = \Pi_{\mathcal{S}(x)} (x^i + \alpha \text{sign}[\nabla_{x^i} l(f_{\theta}(x^i), y)]) \quad (2)$$

Where x^0 is chosen at random from within $\mathcal{S}(x)$, $\Pi_{\mathcal{S}(x)}(\cdot)$ represents the projection into set $\mathcal{S}(x)$, and the adversarial example is obtained after N steps as $x' = x^N$. Here, κ is set to $\epsilon/255$ where ϵ is an integer (usually, $8/255$ for L_{∞} perturbations). For a fair comparison, we set $\alpha = \frac{\epsilon}{8} \times \frac{2}{255}$ which takes the usual value of $\frac{2}{255}$ at $\epsilon = 8$ (Madry et al., 2018). Many variants of PGD-AT have been proposed (Croce et al., 2022; Zhang et al., 2019; Carmon et al., 2019; Kang et al., 2021; Huang et al., 2021; Wu et al., 2021; Rade & Moosavi-Dezfooli, 2021; Pang et al., 2022; Sehwag et al., 2021). In this work, for a rigorous study, we focus on the foundational method without the modifications. We refer to PGD-AT simply as AT throughout this paper.

2.2. Notations

Throughout this work, following Madry et al. (2018) and for brevity, we refer to models trained as described above with perturbation strength $\epsilon/255$ as ϵ -robust models. We denote an N step PGD attack of strength δ as PGD $_{\delta}$ -N.

2.3. Adaptive Attacks

When an improvement to AT is obtained through obfuscated gradients, adaptive attacks are necessary for evaluating the defense. Particularly, when a defense is not differentiable (such as with a scaled floor function in a quantization transformation), the Backward Pass Differentiable Approximation (BPDA) attack (Athalye et al., 2018) is utilized where the non-differentiable defense is usually approximated with an identity function on the backward pass to compute gradients for an attack. Recent work (Croce et al., 2022) also recommends evaluating defenses that adapt models (including their intermediate features) against Transfer PGD, *i.e.*, attacked images obtained from a PGD attack on just the model applied to the adapted model.

3. Overdesigning for Robust Generalization

Motivation: In a typical white-box attack case the attacker has full knowledge of the internal model parameters and training hyperparameters. Post AT, the test and training perturbations respect a fixed ϵ contract on the attack strength. In this section we investigate : *Does deviating from the norm, in terms of attack-strength contracts, impact the overall robustness of the model?*

Experiments: We adversarial train multiple robust models with increasing values of the parameter ϵ and evaluate the models against PGD attacks of increasing strength δ . The clean and robust accuracy along with the hyperparameters used, are given in Appendix A. The various ϵ -robust models have similar clean accuracies, around 85%. We study the variation of errors (100 - accuracy) of the ϵ -robust models on PGD $_{\delta}$ -20 attacks for various $\delta > 0$. We show the plots of robust errors for ϵ -robust models (from $\epsilon = 0$ to 12) with

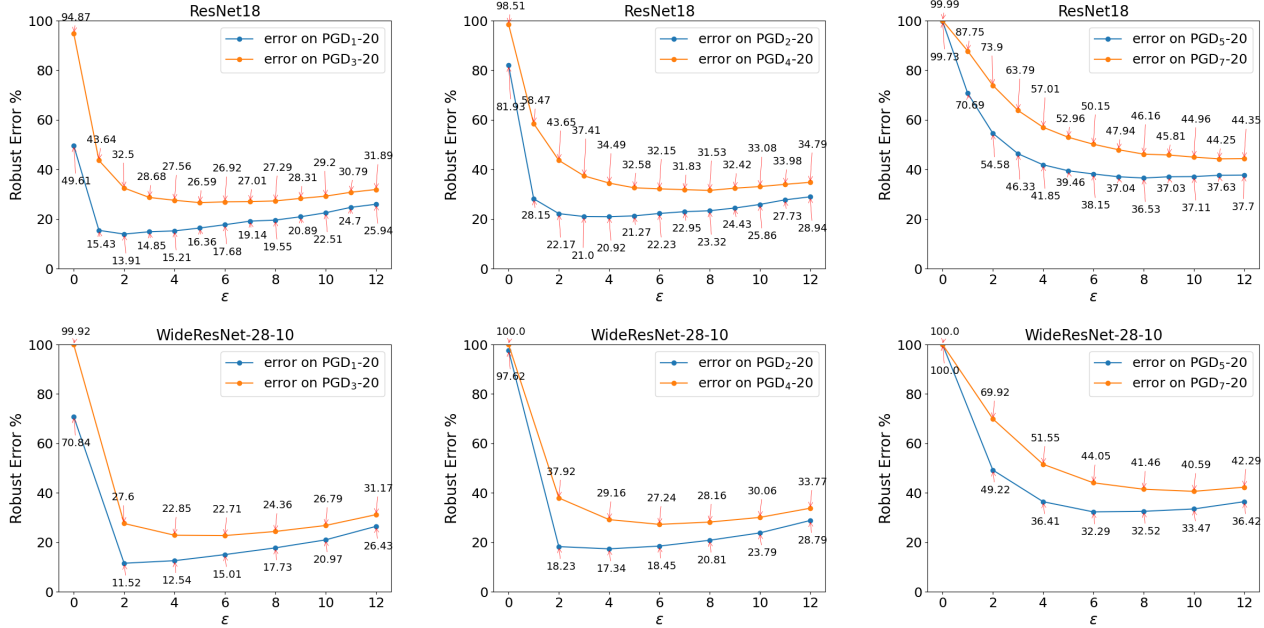


Figure 1: Robust error (= error on $\text{PGD}_{\delta-20}$ on test set) of increasingly ϵ -robust ResNet18 models for $\delta \in \{1, 3\}$ (top left), $\delta \in \{2, 4\}$ (top middle), $\delta \in \{5, 7\}$ (top right), and for WideResNet-28-10 models at $\delta \in \{1, 3\}$ (bottom left), $\delta \in \{2, 4\}$ (bottom middle), and $\delta \in \{5, 7\}$ (bottom right).

$\delta \in \{1, 3\}$, $\delta \in \{2, 4\}$ and $\delta \in \{5, 7\}$ for ResNet18 and WideResNet-28-10 models in Figure 1. We plot the errors for other values of δ in Appendix D.

Discussions: In Figure 1, each curve represents the robust error against a PGD attack at a particular perturbation strength δ . We notice that all four curves have a minima at $\epsilon > \delta$. For instance, in ResNet18 (Figure 1 top row), the 2-robust model generalizes best to the PGD_{1-20} attack ($\epsilon_* - \delta = 1$); the 4-robust model generalizes best to the PGD_{2-20} attack ($\epsilon_* - \delta = 2$); the 5-robust model generalizes best to the PGD_{3-20} attack ($\epsilon_* - \delta = 2$); the 8-robust model generalizes best to the PGD_{4-20} attack ($\epsilon_* - \delta = 4$); the 9-robust model generalizes best to the PGD_{5-20} attack ($\epsilon_* - \delta = 4$); the 11-robust model generalizes best to the PGD_{6-20} attack ($\epsilon_* - \delta = 6$), and so on. Similar behaviour is seen for WideResNet-28-10 models (Figure 1 bottom row).

This is surprising because, one would typically expect that a model trained with the largest ϵ should generalize best to all attacks of strength $\delta \leq \epsilon$. Especially when the clean accuracies are mostly similar. In contrast, the largest ϵ -robust ResNet18 model above (*i.e.*, the 12-robust model) has up to an 8% larger error than the ϵ_* -robust model. Further, from above, we observe that $(\epsilon_* - \delta)$ increases with increasing δ . This implies that eventually for very large δ , the expected notion of the largest ϵ -robust model generalizing best will be true. But at this large value of δ , the perturbations would

no longer be imperceptible to the human eye.

Based on the aforementioned analysis, we suggest *overdesigning* a defense by training models at $\epsilon > \delta$ until an increase in error is seen. For instance, in the case of ResNet18, the ϵ_* -robust models for each δ listed above would be the right choice as the overdesigned model.

4. Intermediate Feature Quantization

Motivation: Quantization offers a simple alternative to induce robustness to input perturbations. Simply on account of the reduced sensitivity to perturbations away from quantization boundaries. There exists some prior work on this in literature, (Buckman et al., 2018; Guo et al., 2017) but have been unable to withstand adaptive attacks like BPDA (Athalye et al., 2018). This seemingly arbitrary defense does seem to have some impact on the robustness of the overall computation. We attempt to study this in more detail here. In particular, we ask the question - *what changes in the intermediate features affect robust accuracy while minimally changing clean accuracy?*

Experiments: We operate at the level of convolutional blocks. We quantize intermediate features after one of the five convolutional blocks in various adversarially trained ResNet18 models, and one of the four blocks in WideResNet-28-10 models. The quantization is performed with a simple element-wise scaled floor function on input tensor $x \in \mathbb{R}^{C \times W \times H}$ given as $\lfloor \beta x_{ijk} \rfloor / \beta$, for some scalar

Analysis of Adversarial Training at a Spectrum of Perturbations

δ	Quantization after layer:	Transf. PGD $_{\delta}$ -20 on ResNet18								BPDA $_{\delta}$ on ResNet18								Transf. PGD $_{\delta}$ -20 on WRN-28-10								BPDA $_{\delta}$ on WRN-28-10							
		ϵ				ϵ				ϵ				ϵ				ϵ				ϵ											
		2	4	8	12	2	4	8	12	2	4	8	12	2	4	8	12	2	4	8	12												
2	none	77.85	79.08	76.69	71.01	77.85	79.08	76.69	71.01	none	81.77	82.67	79.19	71.2	81.77	82.67	79.19	71.2	81.77	82.67	79.19	71.2											
	conv0	79.03	79.42	75.88	68.9	77.29	78.29	75.25	68.41	init conv	81.63	82.76	79.06	70.9	81.62	82.76	79.13	70.9	81.62	82.76	79.13	70.9											
	layer1	78.43	79.31	76.46	70.3	78.0	79.07	76.38	70.28	layer[0]	81.85	82.6	78.92	70.92	81.85	82.62	78.93	70.98	81.85	82.62	78.93	70.98											
	layer2	78.01	79.31	76.71	70.15	77.85	79.15	76.53	70.14	layer[1]	81.72	82.76	79.01	70.46	81.74	82.74	79.02	70.5	81.74	82.74	79.02	70.5											
	layer3	77.84	79.5	76.72	70.97	77.86	79.42	76.71	70.95	layer[2]	81.68	82.74	79.0	70.78	81.74	82.78	79.11	70.9	81.74	82.78	79.11	70.9											
layer4	77.92	79.14	76.69	70.58	77.93	79.2	76.91	70.79																									
4	none	56.39	65.46	68.5	65.2	56.39	65.46	68.5	65.2	none	62.12	70.87	71.81	66.2	62.12	70.87	71.81	66.2	62.12	70.87	71.81	66.2											
	conv0	61.4	67.61	68.23	63.99	57.47	65.27	67.18	62.92	init conv	61.86	70.83	71.53	65.87	61.73	70.8	71.53	65.81	61.73	70.8	71.53	65.81											
	layer1	57.57	66.23	68.28	64.95	56.88	65.72	68.12	64.87	layer[0]	62.43	70.9	71.78	65.97	62.39	70.95	71.82	66.06	62.39	70.95	71.82	66.06											
	layer2	57.12	66.09	68.52	64.78	56.53	65.85	68.23	64.85	layer[1]	62.12	70.92	71.74	65.82	62.14	70.9	71.82	65.82	62.14	70.9	71.82	65.82											
	layer3	56.73	65.84	68.83	65.37	56.59	65.82	68.54	65.55	layer[2]	62.15	70.9	71.77	65.7	62.17	71.04	71.9	65.88	62.17	71.04	71.9	65.88											
layer4	56.54	65.52	68.25	65.2	56.49	65.61	68.51	65.65																									
6	none	35.31	50.31	58.6	58.97	35.31	50.31	58.6	58.97	none	39.5	56.25	62.91	60.54	39.5	56.25	62.91	60.54	39.5	56.25	62.91	60.54											
	conv0	41.13	54.46	60.0	58.61	36.85	51.45	58.22	57.49	init conv	39.4	56.28	62.92	60.61	39.3	56.19	62.95	60.72	39.3	56.19	62.95	60.72											
	layer1	36.22	51.55	58.85	59.06	35.43	50.91	58.7	58.83	layer[0]	40.42	56.73	62.88	60.48	40.28	56.61	63.01	60.59	40.28	56.61	63.01	60.59											
	layer2	36.04	50.99	58.83	59.12	35.61	50.8	58.59	59.18	layer[1]	39.75	56.42	62.96	60.26	39.73	56.33	62.98	60.44	39.73	56.33	62.98	60.44											
	layer3	35.38	50.6	58.99	59.47	35.19	50.68	58.9	59.68	layer[2]	39.54	56.26	62.94	60.45	39.61	56.32	63.23	60.76	39.61	56.32	63.23	60.76											
layer4	35.29	50.39	58.54	58.82	35.32	50.41	59.04	59.65																									
8	none	19.37	36.2	48.77	52.53	19.37	36.2	48.77	52.53	none	22.08	41.2	53.72	54.67	22.08	41.2	53.72	54.67	22.08	41.2	53.72	54.67											
	conv0	24.48	40.58	51.0	52.87	20.78	37.4	48.74	51.15	init conv	21.88	41.26	53.8	54.34	21.88	41.17	53.84	54.46	21.88	41.17	53.84	54.46											
	layer1	19.82	37.31	49.36	52.45	19.38	36.82	49.28	52.41	layer[0]	22.75	41.74	53.92	54.42	22.56	41.69	54.13	54.69	22.56	41.69	54.13	54.69											
	layer2	19.88	36.93	49.43	52.74	19.61	36.6	49.33	52.9	layer[1]	22.24	41.39	53.94	54.49	22.12	41.43	54.07	54.57	22.12	41.43	54.07	54.57											
	layer3	19.42	36.42	49.56	52.86	19.38	36.32	49.58	53.06	layer[2]	22.01	41.21	53.77	54.62	22.14	41.33	54.09	54.99	22.14	41.33	54.09	54.99											
layer4	19.38	36.19	48.84	52.41	19.3	36.29	49.56	53.42																									
10	none	9.63	24.41	39.64	45.67	9.63	24.41	39.64	45.67	none	11.15	28.19	44.65	48.12	11.15	28.19	44.65	48.12	11.15	28.19	44.65	48.12											
	conv0	13.15	28.58	41.99	46.93	10.67	25.17	39.29	44.87	init conv	10.89	28.28	44.58	48.34	11.11	28.13	44.64	48.34	11.11	28.13	44.64	48.34											
	layer1	10.01	25.38	40.31	45.87	9.68	25.01	40.21	45.73	layer[0]	11.69	28.84	45.02	48.45	11.44	28.55	45.0	48.7	11.44	28.55	45.0	48.7											
	layer2	9.9	24.99	40.46	45.91	9.75	24.8	40.26	46.34	layer[1]	11.23	28.47	44.82	48.66	11.02	28.32	44.86	48.76	11.02	28.32	44.86	48.76											
	layer3	9.52	24.59	40.15	45.91	9.25	24.53	40.28	46.1	layer[2]	11.15	28.34	44.61	48.2	11.09	28.37	44.84	48.64	11.09	28.37	44.84	48.64											
layer4	9.69	24.42	39.66	45.55	9.52	24.55	40.49	46.96																									
12	none	4.28	15.48	31.17	39.27	4.28	15.48	31.17	39.27	none	5.18	17.54	35.93	42.09	5.18	17.54	35.93	42.09	5.18	17.54	35.93	42.09											
	conv0	6.51	18.79	33.62	40.74	5.28	16.1	30.85	38.76	init conv	5.08	17.62	35.79	42.06	5.15	17.66	35.84	42.2	5.15	17.66	35.84	42.2											
	layer1	4.42	16.13	31.77	39.54	4.29	15.6	31.56	39.57	layer[0]	5.35	18.19	36.18	42.21	5.35	18.44	36.31	42.42	5.35	18.44	36.31	42.42											
	layer2	4.5	16.11	32.05	39.91	4.37	15.79	31.95	40.43	layer[1]	5.25	17.85	36.34	42.38	5.14	17.9	36.45	42.59	5.14	17.9	36.45	42.59											
	layer3	4.3	15.62	31.72	39.52	4.29	15.52	31.91	39.66	layer[2]	5.15	17.63	36.22	42.26	5.03	17.72	36.49	42.65	5.03	17.72	36.49	42.65											
layer4	4.3	15.45	31.16	39.02	4.34	15.63	31.76	40.36																									

Table 1: Evaluation of quantization on intermediate features of ϵ -robust ResNet18 and WideResNet-28-10 models on the Transfer PGD $_{\delta}$ -20 and BPDA $_{\delta}$ attacks for various ϵ and δ . The intensity of colors in the shaded cells is in proportion to the magnitude of increase over the non-quantized accuracies.

β . Notice that the above operation can be done for any intermediate neuron in the DNN, and can be prohibitively large to explore in an individual basis. But, a useful abstraction is to work at the level of layers of the DNN. We evaluate feature-quantization on two adaptive attacks, namely, BPDA $_{\delta}$ from Athalye et al. (2018) and Transfer PGD $_{\delta}$ -20 from Croce et al. (2022) for various δ 's and show some sample results in Table 1. The complete set of results for $\epsilon \in [0, 12]$ and $\delta \in \{0, 2, 4, 6, 8\}$, clean accuracies after quantization and ablations for various β values can be found in Appendix C.

Discussions: In Table 1, the cells shaded blue represent an increase over the unquantized model (gray cells) while, cells shaded red denote a loss in accuracy. The dark blue shaded lines in Table 1 correspond to accuracies obtained with quantization after ‘conv0’ for ResNet18 and after ‘layer[0]’ for WideResNet-28-10. They denote significant increase in accuracy with quantization of intermediate features after the first layer in ResNet18 and after the second layer in WideResNet-28-10. Whereas, the red shaded cells on the top right show a loss in robustness on the weak attack $\delta = 2$ for high strength ($\epsilon = 8, \dots, 12$) models. This can be understood as the expected (but minimal) loss in accuracy with a drop in resolution for features of attacked

images that are almost the same as clean images.

Unexpectedly, we also notice that the shaded blue values span across seen ($\epsilon \geq \delta$) and unseen attacks ($\epsilon < \delta$). Further, with individual columns of ϵ -robust models like the $\epsilon = 12$ column under the transfer PGD attack on WRN-28-10 and the $\epsilon = 2$ column under the BPDA attack on WRN-28-10, it would have been easy to reject this technique as unsuitable. Yet, with an evaluation spanning across increasing values of ϵ , we notice that broad improvements are attained in both seen and unseen attacks, other columns of Table 1. Our evaluation confirms that quantization can be applied to any model to provide both seen and unseen robustness without explicit calibration to unseen attacks.

5. AT and Norm of CNN Kernels

Motivation: In this section we attempt to analyze the variation in the norm of the kernel weights for different layers across increasingly robust models. The kernel weights are square matrices of shape 3×3 . Each convolutional operation in a CNN computes an output of the form $y = w^T v$, where $\{w, v\} \in \mathbb{R}^d$ and $d = 9$. v represents the part of the input the kernel gets applied to. Then by Cauchy-Schwartz inequality $\|y\| = \|w^T v\| \leq \|w\| \|v\|$. The norm $\|w\|_{\infty} = \max_i |w_i|$ serves as the L_{∞} Lipschitz constant

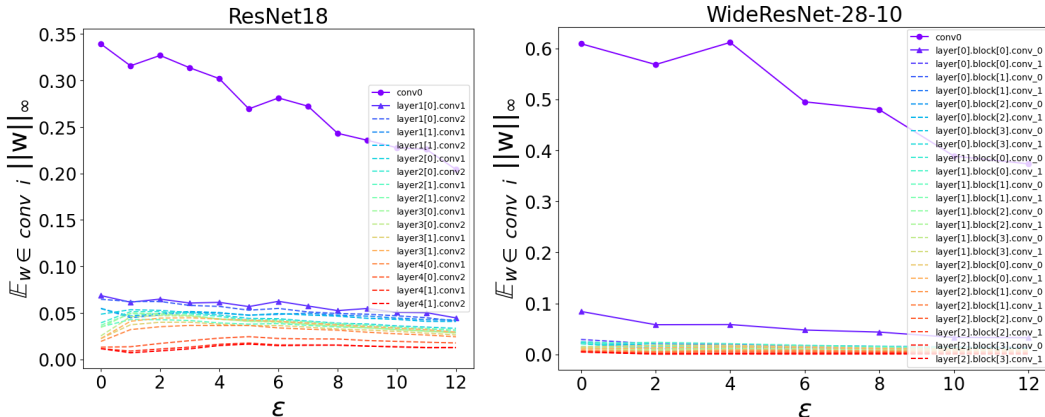


Figure 2: Plot of maximum of L_∞ norms of filters in various layers for increasingly ϵ -robust ResNet18 (left) and WideResNet-28-10 (right) models.

Model	non-robust	1	2	3	4	5	6	7	8	9	10	11	12
ResNet18	66.0	<u>81.8</u>	81.97	81.28	80.19	79.07	77.83	76.33	75.46	74.14	72.62	70.82	69.37
WideResNet-28-10	58.48	-	84.0	-	82.49	-	79.74	-	76.68	-	73.53	-	68.48

Table 2: Average accuracy of ϵ -robust ResNet18 and WideResNet-28-10 models (for various ϵ) on all common corruptions in CIFAR-10-C dataset. The bold and underlined values denote the largest and second largest value in each row.

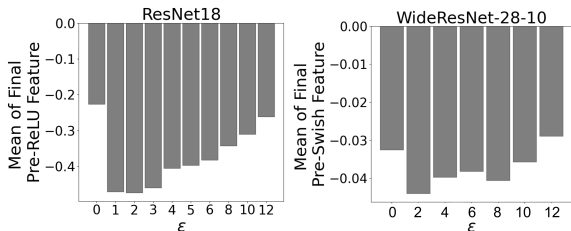


Figure 3: Mean of Final Pre-ReLU / Pre-Swish features for increasingly robust ResNet18 (left) and WideResNet-28-10 (right) models.

for y w.r.t to the input v . Thus, we analyze the L_∞ norm of kernel weights to study the sensitivity of convolutional layers to L_∞ norm bounded perturbations.

Experiments: We analyze the average and worst case performance for each layer in ResNet18 and WideResNet-28-10 models, by analyzing the average filter sensitivity and the filter that is most sensitive to input perturbations respectively. These can be measured by the average and maximum over the filter norms in each layer. That is, for a particular convolution layer i , we compute $\mathbb{E}_{w \in \text{conv}_i} \|w\|_\infty$ and $\max_{w \in \text{conv}_i} \|w\|_\infty$. We plot the former for each layer of increasingly ϵ -robust ResNet18 and WideResNet-28-10 models in Figure 2 and the latter in Appendix D.

Discussions: We observe in Figure 2, the first two curves which denote the average L_∞ Lipschitz constant of filters in the first two layers of ResNet18, take much larger values when compared to the curves corresponding to the rest of the layers. The large separation between the first two layers

and remaining layers is again observed for WideResNet-28-10. The plot of maximum L_∞ Lipschitz constant of filters of each layer in Appendix D also displays a similar separation between the first two layers and other layers. Moreover, it depicts that the curves of the first and second layer monotonically increase for ResNet18 but not for WideResNet-28-10. From the above, we infer the following: (1) the first two layers are primarily responsible for propagating perturbations from input to output, and (2) wider networks may realize greater adversarial robustness from implicit regularization of their first two layers. Further, our conclusion on the filter’s L_∞ Lipschitz constants of the first two layers playing an outsized role, agrees with our previous observations in Section 4. Where, quantization of intermediate features after these layers provided the greatest increases in accuracy. This leads us to the following conjecture: the first two layers play an important role in robustness compared to the other layers. When designing robust techniques, special attention needs to be devoted to these layers in order to have a far reaching impact.

6. Training with Larger Perturbations and Common-Corruptions

Motivation: While training with a spectrum of ϵ values can uncover new techniques, otherwise not apparent at a single ϵ , it can have potential downsides. An alternate way to assess the robustness of a DNN model is to evaluate on common corruptions like image noise. When trained in an adversarial setting we expect the following - AT, albeit unintentionally, should increase the general robustness of

the model against corruptions like Gaussian noise, weather shifts and alike as discussed in Hendrycks & Dietterich (2019). Even though AT is a standard comparison benchmark when it comes to techniques for increasing robustness in such common corruptions setting, the further analysis into testing the limits of this is often overlooked. The only work that tests the limits (Kireev et al., 2021) has previously reported that 1-robust models perform better than 8-robust models.

Experiments: To this end, we test increasingly robust models on images with common corruptions from the CIFAR-10-C dataset (Hendrycks & Dietterich, 2019). The complete results on each corruption is in Appendix E. We present the average accuracy across the full dataset in Table 2. We notice another facet of perturbation strength - models trained with smaller ϵ 's obtain better robustness across all kinds of corruptions – which is not what one would expect. Further, the accuracy on corrupted images uniformly decreases after $\epsilon = 1$ or 2 on almost all corruptions. On average, the 2-robust models have the highest robustness (for both ResNet18 and WideResNet-28-10), followed by the 1-robust model for ResNet18 and the 4-robust model for WideResNet-28-10.

Discussions: We understand this peculiar behaviour in terms of the features before ReLU functions and in particular the final Pre-ReLU/Pre-Swish features. Unlike adversarial attacked images which have small bounded perturbations, corrupted images, have numerically larger perturbations. These perturbations when propagated through the model are more likely to flip an input to a ReLU neuron from negative to positive (or vice versa) when it is closer to zero. Consequently, we notice that the mean of the final pre-ReLU features (for ResNet18) and pre-Swish features (for WideResNet-28-10) on the complete CIFAR-10-C dataset are further away from zero for lower strength models (see Figure 3). The highly biased positions of these final pre-activation features is likely to be responsible for the increased robustness of the lower ϵ -robust models. Moreover, this reveals that it may not always be helpful to train with increasing ϵ , particularly from the vantage point of images corrupted with common noise.

7. Related Work

AT has been discussed in a vast body of work. Here, we only describe literature relevant to our findings.

On varying perturbation strength in AT: On the attack side, recent papers have explored robustness to unseen attacks (Stutz et al., 2020; Laidlaw et al., 2020). Our proposed quantization is complementary to these methods (and standard AT and its variants) and unlike these methods does not explicitly need to be calibrated to unseen attacks.

For defenses, while few papers (Balaji et al., 2019; Cheng et al., 2020; Ding et al., 2018) have proposed AT algorithms that utilize varying perturbation strengths for each sample, they are still usually constrained by an upper bound on perturbation strength. Thus, these works are still restricted to feedback from a model when trained within that upper bound. As far as we are aware, there is a dearth of work that employs feedback from a spectrum of perturbation strengths or upper bounds to improve AT. In future work, we plan to execute the aforementioned perturbation-customized algorithms at various upper bounds to gain further insight into improvements for AT.

On quantization: Quantization and transformations of input images have been explored in Buckman et al. (2018); Guo et al. (2017) but are only able to provide robustness gains because of obfuscated gradients, and hence are unable to stand against an adaptive BPDA attack (Athalye et al., 2018). Further, recent work on intermediate feature transformations based on Neural ODEs (Kang et al., 2021; Chen et al., 2021) have been shown to also not provide any additional benefits against adaptive attacks (Croce et al., 2022). In contrast, by simply applying quantization, we improve robustness against both BPDA and Transfer PGD.

On convolution filters and AT: Concurrent work (Gavrikov & Keuper, 2022) has analyzed robust models from the viewpoint of the models' convolution filters. They analyze the sparsity and diversity of filters to conclude that the first layer plays a very important role. While we concur with their analysis of the importance of the first layer, we identify exactly how the first layer contributes to perturbation propagation by analyzing filter norms across a spectrum of perturbation strengths. Further, we identify, again across various perturbations strengths, that the second layer appears just as important through both the filter norms and the effect of quantization after both layers.

8. Conclusions and Future Work

In this paper, we analyzed AT models trained at a spectrum of perturbation strengths and identified new techniques (overdesigning, quantization, sensitivity of convolutional filter weights) not apparent from standard analysis at just a single defense perturbation strength. We explored the effects of these techniques on adversarial robustness of ResNet and WideResNet models to seen and unseen, standard and adaptive attacks on CIFAR-10. Finally, we discovered a potential downside to training at various perturbation strengths, in the form of a drop in robustness to common corruptions. In future work, we aim to study perturbation-customized AT variants and test-time defenses at a spectrum of perturbations, and identify methods to regularize the first two layers to further improve robustness in AT models.

References

- Athalye, A., Carlini, N., and Wagner, D. Obfuscated gradients give a false sense of security: Circumventing defenses to adversarial examples. In *International conference on machine learning*, pp. 274–283. PMLR, 2018.
- Balaji, Y., Goldstein, T., and Hoffman, J. Instance adaptive adversarial training: Improved accuracy tradeoffs in neural nets. *arXiv preprint arXiv:1910.08051*, 2019.
- Buckman, J., Roy, A., Raffel, C., and Goodfellow, I. Thermometer encoding: One hot way to resist adversarial examples. In *International Conference on Learning Representations*, 2018.
- Carmon, Y., Raghunathan, A., Schmidt, L., Duchi, J. C., and Liang, P. S. Unlabeled data improves adversarial robustness. *Advances in Neural Information Processing Systems*, 32, 2019.
- Chen, Z., Li, Q., and Zhang, Z. Towards robust neural networks via close-loop control. *arXiv preprint arXiv:2102.01862*, 2021.
- Cheng, M., Lei, Q., Chen, P.-Y., Dhillon, I., and Hsieh, C.-J. Cat: Customized adversarial training for improved robustness. *arXiv preprint arXiv:2002.06789*, 2020.
- Croce, F., Andriushchenko, M., Sehwag, V., Debenedetti, E., Flammarion, N., Chiang, M., Mittal, P., and Hein, M. Robustbench: a standardized adversarial robustness benchmark. *arXiv preprint arXiv:2010.09670*, 2020.
- Croce, F., Goyal, S., Brunner, T., Shelhamer, E., Hein, M., and Cemgil, T. Evaluating the adversarial robustness of adaptive test-time defenses. *arXiv preprint arXiv:2202.13711*, 2022.
- Ding, G. W., Sharma, Y., Lui, K. Y. C., and Huang, R. Mma training: Direct input space margin maximization through adversarial training. *arXiv preprint arXiv:1812.02637*, 2018.
- Gavrikov, P. and Keuper, J. Adversarial robustness through the lens of convolutional filters. *arXiv preprint arXiv:2204.02481*, 2022.
- Goyal, S., Qin, C., Uesato, J., Mann, T., and Kohli, P. Uncovering the limits of adversarial training against norm-bounded adversarial examples. *arXiv preprint arXiv:2010.03593*, 2020.
- Goyal, S., Rebuffi, S.-A., Wiles, O., Stimberg, F., Calian, D. A., and Mann, T. A. Improving robustness using generated data. *Advances in Neural Information Processing Systems*, 34, 2021.
- Guo, C., Rana, M., Cisse, M., and Van Der Maaten, L. Countering adversarial images using input transformations. *arXiv preprint arXiv:1711.00117*, 2017.
- Hendrycks, D. and Dietterich, T. Benchmarking neural network robustness to common corruptions and perturbations. *arXiv preprint arXiv:1903.12261*, 2019.
- Huang, H., Wang, Y., Erfani, S., Gu, Q., Bailey, J., and Ma, X. Exploring architectural ingredients of adversarially robust deep neural networks. *Advances in Neural Information Processing Systems*, 34, 2021.
- Kang, Q., Song, Y., Ding, Q., and Tay, W. P. Stable neural ode with lyapunov-stable equilibrium points for defending against adversarial attacks. *Advances in Neural Information Processing Systems*, 34, 2021.
- Kireev, K., Andriushchenko, M., and Flammarion, N. On the effectiveness of adversarial training against common corruptions. *arXiv preprint arXiv:2103.02325*, 2021.
- Laidlaw, C., Singla, S., and Feizi, S. Perceptual adversarial robustness: Defense against unseen threat models. *arXiv preprint arXiv:2006.12655*, 2020.
- Madry, A., Makelov, A., Schmidt, L., Tsipras, D., and Vladu, A. Towards deep learning models resistant to adversarial attacks. In *International Conference on Learning Representations*, 2018. URL <https://openreview.net/forum?id=rJzIBfZAb>.
- Pang, T., Yang, X., Dong, Y., Su, H., and Zhu, J. Bag of tricks for adversarial training. *arXiv preprint arXiv:2010.00467*, 2020.
- Pang, T., Lin, M., Yang, X., Zhu, J., and Yan, S. Robustness and accuracy could be reconcilable by (proper) definition. *arXiv preprint arXiv:2202.10103*, 2022.
- Rade, R. and Moosavi-Dezfooli, S.-M. Helper-based adversarial training: Reducing excessive margin to achieve a better accuracy vs. robustness trade-off. In *ICML 2021 Workshop on Adversarial Machine Learning*, 2021.
- Rebuffi, S.-A., Goyal, S., Calian, D. A., Stimberg, F., Wiles, O., and Mann, T. Fixing data augmentation to improve adversarial robustness. *arXiv preprint arXiv:2103.01946*, 2021.
- Sehwag, V., Mahloujifar, S., Handina, T., Dai, S., Xiang, C., Chiang, M., and Mittal, P. Robust learning meets generative models: Can proxy distributions improve adversarial robustness? *arXiv preprint arXiv:2104.09425*, 2021.
- Sridhar, K., Sokolsky, O., Lee, I., and Weimer, J. Improving neural network robustness via persistency of excitation. *arXiv preprint arXiv:2106.02078*, 2021.

Stutz, D., Hein, M., and Schiele, B. Confidence-calibrated adversarial training: Generalizing to unseen attacks. In *International Conference on Machine Learning*, pp. 9155–9166. PMLR, 2020.

Wu, B., Chen, J., Cai, D., He, X., and Gu, Q. Do wider neural networks really help adversarial robustness? *Advances in Neural Information Processing Systems*, 34, 2021.

Xie, C. and Yuille, A. Intriguing properties of adversarial training at scale. *arXiv preprint arXiv:1906.03787*, 2019.

Zhang, H., Yu, Y., Jiao, J., Xing, E., El Ghaoui, L., and Jordan, M. Theoretically principled trade-off between robustness and accuracy. In *International conference on machine learning*, pp. 7472–7482. PMLR, 2019.

Appendix: Experimental Details and Additional Results

Our code and models can be found at the following link: https://github.com/perturb-spectrum/analysis_and_methods.

A. Adversarially Trained Models' Performance and Hyperparameters

A.1. Adversarially Trained Models

Accuracy (%)	ϵ												
	0	1	2	3	4	5	6	7	8	9	10	11	12
clean	85.58	88.25	88.79	88.16	88.09	87.95	86.35	84.66	84.63	83.23	83.32	83.33	83.5
PGD $_{\epsilon}$ -20	85.58	84.57	77.83	71.32	65.51	60.54	55.71	52.06	48.75	45.56	43.16	41.69	39.06

Table 3: Clean and adversarial performance of ResNet-18 models on increasing values of ϵ .

Accuracy (%)	ϵ						
	0	2	4	6	8	10	12
clean	85.45	88.41	88.13	88.66	85.23	83.51	82.83
PGD $_{\epsilon}$ -20	85.45	81.77	70.84	62.03	53.75	47.54	42.17

Table 4: Clean and adversarial performance of WideResNet-28-10 models on increasing values of ϵ .

Hyperparameter	ResNet18		WideResNet-28-10	
	Standard Training	AT	Standard Training	AT
batch size	512	256	512	128
optimizer	SGD with momentum=0.9 and weight decay= 2×10^{-4}			
learning rate schedule	starting at 0.1 and divided by 10 at epochs 75, 90, and 100.			
PGD Step Size	-	$\frac{2}{8} \times \frac{2}{255}$	-	$\frac{2}{8} \times \frac{2}{255}$
PGD Random Start	-	True	-	True
total epochs	50	200	50	200
epoch of best checkpoint	19	76	18	80

Table 5: Hyperparameters for Standard and AT with ResNet18 and WideResNet-28-10.

B. Overdesigning for Robust Generalization

Figure 4 depicts the robust error for increasingly ϵ -robust ResNet18 and WideResNet-28 at attack perturbation strengths $\delta = 6$ and 8. The trend is similar to Figure 1. Specifically, we notice that the 9-robust model generalizes best to PGD $_{\delta}$ -20 for ResNet18; the 10-robust model generalizes best to PGD $_{\delta}$ -20 for WideResNet-28-10 continuing the trend in $\epsilon_{\text{best}} - \delta$ discussed in Section 3.

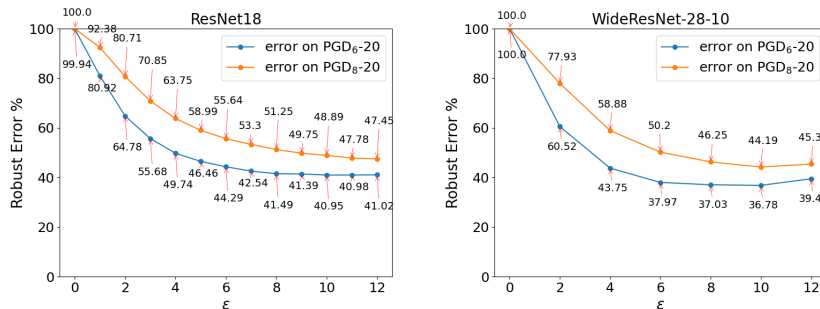


Figure 4: Robust error (= error on PGD $_{\delta}$ -20 on test set) of increasingly ϵ -robust ResNet18 (left) and WideResNet-28-10 (right) models for $\delta \in \{6, 8\}$.

C. Intermediate feature Quantization

C.1. BPDA

We table the complete set of accuracies of ϵ robust ResNet18 and WideResNet-28-10 models on BPDA $_{\delta}$, for various ϵ and δ , in Tables 6 and 7 respectively.

δ	Quant. after layer:	ϵ												
		0	1	2	3	4	5	6	7	8	9	10	11	12
2	none	18.15	71.84	77.85	79.01	79.08	78.75	77.77	77.05	76.69	75.57	74.13	72.28	71.01
	conv0	21.04	71.53	77.29	77.92	78.29	77.96	76.15	75.36	75.25	73.98	71.28	69.54	68.41
	layer1	17.57	71.78	78.00	79.05	79.07	78.77	77.67	76.66	76.38	74.62	73.61	71.78	70.28
	layer2	18.21	71.90	77.85	78.84	79.15	78.64	77.81	76.96	76.53	75.59	73.44	71.74	70.14
	layer3	18.04	72.11	77.86	78.88	79.42	78.86	77.87	77.14	76.71	75.81	74.17	72.49	70.95
layer4	18.20	72.04	77.93	79.00	79.20	78.58	77.67	77.05	76.91	75.64	74.11	72.33	70.79	
4	none	1.49	41.50	56.39	62.54	65.46	67.42	67.82	68.16	68.50	67.61	66.88	66.08	65.20
	conv0	2.26	44.01	57.47	62.95	65.27	66.65	66.54	66.80	67.18	66.24	64.32	63.37	62.92
	layer1	1.35	41.72	56.88	62.90	65.72	67.40	67.89	68.06	68.12	67.10	66.63	65.50	64.87
	layer2	1.47	41.82	56.53	62.70	65.85	67.68	68.03	68.02	68.23	67.60	66.65	65.72	64.85
	layer3	1.45	41.54	56.59	62.68	65.82	67.67	68.02	68.61	68.54	67.97	67.28	66.15	65.55
layer4	1.47	41.73	56.49	62.70	65.61	67.48	67.90	68.21	68.51	67.81	67.08	66.29	65.65	
6	none	0.05	19.10	35.31	44.50	50.31	53.50	55.59	57.45	58.60	58.66	59.12	59.03	58.97
	conv0	0.16	21.23	36.85	45.87	51.45	54.26	55.77	57.02	58.22	57.93	57.11	57.18	57.49
	layer1	0.08	19.04	35.43	45.20	50.91	54.12	56.01	57.63	58.70	58.60	58.90	58.97	58.83
	layer2	0.04	19.08	35.61	44.74	50.80	53.85	55.91	57.67	58.59	59.04	59.05	59.21	59.18
	layer3	0.05	19.18	35.19	44.90	50.68	53.94	56.05	57.84	58.90	59.13	59.47	59.33	59.68
layer4	0.05	19.31	35.32	44.45	50.41	53.80	56.01	57.67	59.04	59.06	59.60	59.69	59.65	
8	none	0.00	7.74	19.37	29.25	36.20	41.00	44.29	46.76	48.77	50.13	51.08	52.21	52.53
	conv0	0.00	8.72	20.78	30.72	37.40	41.65	44.37	46.77	48.74	50.05	50.01	50.57	51.15
	layer1	0.00	7.51	19.38	29.79	36.82	41.61	44.78	47.02	49.28	50.32	51.15	52.44	52.41
	layer2	0.00	7.55	19.61	29.22	36.60	41.59	44.95	47.40	49.33	50.64	51.54	52.50	52.90
	layer3	0.00	7.28	19.38	29.53	36.32	41.51	44.78	47.60	49.58	50.53	51.63	52.63	53.06
layer4	0.00	7.62	19.30	29.19	36.29	41.34	44.70	47.28	49.56	50.78	51.73	52.77	53.42	
10	none	0.00	2.66	9.63	17.81	24.41	29.79	33.58	36.81	39.64	41.57	43.21	45.14	45.67
	conv0	0.00	3.12	10.67	18.83	25.17	30.23	34.15	37.08	39.29	41.71	42.57	43.69	44.87
	layer1	0.00	2.53	9.68	18.20	25.01	30.33	34.26	37.16	40.21	41.79	43.35	45.33	45.73
	layer2	0.00	2.58	9.75	17.98	24.80	30.11	34.10	37.73	40.26	42.39	43.96	45.93	46.34
	layer3	0.00	2.59	9.25	17.91	24.53	30.37	34.20	37.56	40.28	42.08	43.87	45.56	46.10
layer4	0.00	2.68	9.52	17.99	24.55	29.76	34.05	37.17	40.49	42.34	44.04	46.22	46.96	
12	none	0.00	0.94	4.28	9.97	15.48	20.20	24.16	27.80	31.17	33.49	35.74	38.05	39.27
	conv0	0.00	1.20	5.28	10.97	16.10	20.99	24.61	27.51	30.85	33.61	35.25	36.74	38.76
	layer1	0.00	0.82	4.29	10.42	15.60	20.78	24.84	28.24	31.56	34.31	36.11	38.81	39.57
	layer2	0.00	0.86	4.37	10.08	15.79	20.63	24.78	28.47	31.95	34.38	36.81	39.22	40.43
	layer3	0.00	0.83	4.29	9.94	15.52	20.38	25.01	28.33	31.91	34.26	36.49	38.56	39.66
layer4	0.00	0.91	4.34	9.97	15.63	20.26	24.62	28.26	31.76	34.43	36.67	39.27	40.36	

Table 6: Evaluation of quantization after four intermediate features of ϵ -robust ResNet-18 models on the BPDA $_{\delta}$ attack for various ϵ and δ at $\beta = 8.0$.

Analysis of Adversarial Training at a Spectrum of Perturbations

δ	Quant. after layer:	ϵ						
		0	2	4	6	8	10	12
2	none	2.43	81.77	82.67	81.58	79.19	76.23	71.20
	init conv	2.48	81.62	82.76	81.62	79.13	75.98	70.90
	layer[0]	2.11	81.85	82.62	81.47	78.93	76.11	70.98
	layer[1]	2.38	81.74	82.74	81.57	79.02	76.06	70.50
	layer[2]	2.41	81.74	82.78	81.49	79.11	76.06	70.90
4	none	0.00	62.12	70.87	72.80	71.81	69.95	66.20
	init conv	0.00	61.73	70.80	72.91	71.53	69.62	65.81
	layer[0]	0.00	62.39	70.95	73.12	71.82	69.74	66.06
	layer[1]	0.00	62.14	70.90	72.88	71.82	69.80	65.82
	layer[2]	0.00	62.17	71.04	72.82	71.90	70.05	65.88
6	none	0.00	39.50	56.25	62.01	62.91	63.28	60.54
	init conv	0.00	39.30	56.19	62.15	62.95	62.90	60.72
	layer[0]	0.00	40.28	56.61	62.13	63.01	63.03	60.59
	layer[1]	0.00	39.73	56.33	62.34	62.98	63.33	60.44
	layer[2]	0.00	39.61	56.32	62.38	63.23	63.50	60.76
8	none	0.00	22.08	41.20	49.83	53.72	55.81	54.67
	init conv	0.00	21.88	41.17	49.76	53.84	55.51	54.46
	layer[0]	0.00	22.56	41.69	49.99	54.13	55.85	54.69
	layer[1]	0.00	22.12	41.43	50.05	54.07	55.69	54.57
	layer[2]	0.00	22.14	41.33	50.00	54.09	55.91	54.99
10	none	0.00	11.15	28.19	38.37	44.65	47.70	48.12
	init conv	0.00	11.11	28.13	38.41	44.64	47.80	48.34
	layer[0]	0.00	11.44	28.55	38.89	45.00	48.16	48.70
	layer[1]	0.00	11.02	28.32	38.88	44.86	47.89	48.76
	layer[2]	0.00	11.09	28.37	38.71	44.84	48.12	48.64
12	none	0.00	5.18	17.54	28.08	35.93	39.84	42.09
	init conv	0.00	5.15	17.66	28.23	35.84	39.90	42.20
	layer[0]	0.00	5.35	18.44	28.62	36.31	39.93	42.42
	layer[1]	0.00	5.14	17.90	28.32	36.45	40.54	42.59
	layer[2]	0.00	5.03	17.72	28.41	36.49	40.40	42.65

Table 7: Evaluation of quantization after four intermediate features of ϵ -robust WideResNet-28-10 models on the BPDA $_{\delta}$ attack for various ϵ and δ at $\beta = 8.0$.

C.2. Transfer PGD with Ablations

We table the complete set of accuracies of ϵ robust ResNet18 and WideResNet-28-10 models on Transfer PGD $_{\delta}$ -20 attack, for various ϵ and δ , at quantization scaling factor of $\beta = 8.0$ in Tables 8 and 13 respectively.

We repeat our experiments with ResNet18 models for quantization scaling factors of $\beta = 6.0, 8.0, 10.0$ and 12.0 and display all accuracies for various ϵ and δ in Tables 9, 10, 11, and 12 respectively.

We repeat our experiments again with WideResNet-28-10 models for quantization scaling factors of $\beta = 6.0, 8.0, 10.0$ and 12.0 and display all accuracies for various ϵ and δ in Tables 14, 15, 16, and 17 respectively.

We continue to observe increase in robustness to seen and unseen BPDA and Transfer PGD in all the below tables.

Analysis of Adversarial Training at a Spectrum of Perturbations

δ	Quant. after layer:	ϵ													
		0	1	2	3	4	5	6	7	8	9	10	11	12	
2	none	18.15	71.84	77.85	79.01	79.08	78.75	77.77	77.05	76.69	75.57	74.13	72.28	71.01	
	conv0	31.83	75.11	79.03	79.36	79.42	78.68	77.20	76.17	75.88	74.43	71.84	70.39	68.90	
	layer1	18.57	72.73	78.43	79.56	79.31	78.98	77.88	76.83	76.46	74.78	73.61	71.82	70.30	
	layer2	18.60	72.38	78.01	79.09	79.31	78.76	77.95	77.00	76.71	75.58	73.48	71.71	70.15	
	layer3	18.29	72.09	77.84	78.89	79.50	78.92	77.97	77.12	76.72	75.83	74.23	72.40	70.97	
4	layer4	18.33	71.89	77.92	78.98	79.14	78.57	77.63	76.97	76.69	75.48	73.82	72.12	70.58	
	none	1.49	41.50	56.39	62.54	65.46	67.42	67.82	68.16	68.50	67.61	66.88	66.08	65.20	
	conv0	4.22	50.03	61.40	66.06	67.61	68.45	68.42	68.63	68.23	67.35	65.66	64.80	63.99	
	layer1	1.41	42.95	57.57	63.64	66.23	67.67	68.04	68.34	68.28	67.29	66.78	65.59	64.95	
	layer2	1.53	42.20	57.12	63.17	66.09	67.77	68.09	68.27	68.52	67.55	66.68	65.68	64.78	
6	layer3	1.45	41.65	56.73	62.82	65.84	67.84	67.98	68.57	68.83	67.92	67.30	66.22	65.37	
	layer4	1.48	41.58	56.54	62.67	65.52	67.41	67.68	68.04	68.25	67.42	66.67	65.84	65.20	
	none	0.05	19.10	35.31	44.50	50.31	53.50	55.59	57.45	58.60	58.66	59.12	59.03	58.97	
	conv0	0.28	26.14	41.13	50.09	54.46	56.68	58.43	59.15	60.00	59.47	59.28	59.16	58.61	
	layer1	0.05	20.13	36.22	45.82	51.55	54.38	56.30	57.91	58.85	58.77	59.02	59.16	59.06	
8	layer2	0.05	19.60	36.04	45.39	50.99	54.15	56.24	58.03	58.83	59.02	59.27	59.31	59.12	
	layer3	0.05	19.29	35.38	45.01	50.60	54.01	56.20	57.79	58.99	58.99	59.36	59.34	59.47	
	layer4	0.05	19.21	35.29	44.50	50.39	53.43	55.57	57.27	58.54	58.47	58.92	58.91	58.82	
	none	0.00	7.74	19.37	29.25	36.20	41.00	44.29	46.76	48.77	50.13	51.08	52.21	52.53	
	conv0	0.00	11.40	24.48	35.10	40.58	44.30	47.55	49.43	51.00	51.74	52.43	52.91	52.87	
10	layer1	0.00	8.07	19.82	30.47	37.31	41.89	45.02	47.34	49.36	50.65	51.22	52.50	52.45	
	layer2	0.00	7.98	19.88	29.88	36.93	41.84	45.12	47.57	49.43	50.60	51.44	52.40	52.74	
	layer3	0.00	7.70	19.42	29.42	36.42	41.40	44.63	47.32	49.56	50.40	51.51	52.42	52.86	
	layer4	0.00	7.72	19.38	29.24	36.19	40.95	44.19	46.81	48.84	50.06	51.13	52.19	52.41	
	none	0.00	2.66	9.63	17.81	24.41	29.79	33.58	36.81	39.64	41.57	43.21	45.14	45.67	
12	conv0	0.00	4.29	13.15	22.37	28.58	33.23	37.69	40.01	41.99	43.85	45.01	46.90	46.93	
	layer1	0.00	2.70	10.01	18.73	25.38	30.60	34.54	37.22	40.31	41.95	43.43	45.48	45.87	
	layer2	0.00	2.75	9.90	18.32	24.99	30.60	34.56	37.65	40.46	42.27	43.97	45.71	45.91	
	layer3	0.00	2.63	9.52	17.91	24.59	30.38	34.02	37.35	40.15	41.97	43.66	45.60	45.91	
	layer4	0.00	2.66	9.69	17.84	24.42	29.72	33.62	36.67	39.66	41.44	43.17	45.19	45.55	
12	none	0.00	0.94	4.28	9.97	15.48	20.20	24.16	27.80	31.17	33.49	35.74	38.05	39.27	
	conv0	0.00	1.56	6.51	13.09	18.79	23.38	27.84	30.85	33.62	36.08	38.04	40.02	40.74	
	layer1	0.00	0.99	4.42	10.63	16.13	21.04	25.00	28.50	31.77	34.46	36.14	38.65	39.54	
	layer2	0.00	0.98	4.50	10.37	16.11	20.66	25.05	28.55	32.05	34.46	36.63	39.09	39.91	
	layer3	0.00	0.94	4.30	10.08	15.62	20.52	24.54	28.27	31.72	34.07	36.13	38.57	39.52	
layer4	0.00	0.94	4.30	10.02	15.45	20.19	24.22	27.91	31.16	33.59	35.92	38.09	39.02		

Table 8: Evaluation of quantization on all four intermediate features of ϵ -robust ResNet18 models on the Transfer PGD $_{\delta}$ -20 attack for various ϵ and δ at $\beta = 8.0$.

δ	Quant. after layer:	ϵ													
		0	1	2	3	4	5	6	7	8	9	10	11	12	
2	none	18.15	71.84	77.85	79.01	79.08	78.75	77.77	77.05	76.69	75.57	74.13	72.28	71.01	
	conv0	39.35	73.15	77.24	77.33	77.04	75.89	73.23	72.37	71.49	69.60	64.05	62.19	62.61	
	layer1	19.00	73.28	78.73	79.63	79.15	78.87	77.73	76.32	75.92	73.68	73.03	70.68	69.14	
	layer2	18.85	72.48	78.33	79.32	79.47	78.92	77.85	76.61	76.16	75.21	72.15	70.76	69.07	
	layer3	18.25	72.09	77.93	79.05	79.61	79.08	78.27	77.16	76.87	75.77	74.45	72.27	70.79	
4	layer4	18.33	71.91	77.81	78.81	79.08	78.57	77.65	76.91	76.67	75.25	73.46	71.88	70.32	
	none	1.49	41.50	56.39	62.54	65.46	67.42	67.82	68.16	68.50	67.61	66.88	66.08	65.20	
	conv0	16.72	56.72	64.91	67.38	67.91	67.77	66.45	65.80	65.59	64.06	59.37	58.38	58.93	
	layer1	1.43	45.81	58.67	64.73	66.82	68.13	68.28	68.34	68.33	66.79	66.53	64.86	63.82	
	layer2	1.59	43.37	58.13	64.03	66.79	68.01	68.24	68.53	68.52	67.62	66.21	64.91	64.19	
6	layer3	1.44	41.97	57.11	63.49	66.52	68.21	68.27	68.84	68.84	68.23	67.48	66.14	65.18	
	layer4	1.50	41.65	56.59	62.56	65.48	67.20	67.75	67.96	68.11	67.08	66.55	65.71	64.85	
	none	0.05	19.10	35.31	44.50	50.31	53.50	55.59	57.45	58.60	58.66	59.12	59.03	58.97	
	conv0	5.40	37.87	49.38	55.65	57.92	58.51	58.89	59.13	58.90	58.06	54.92	54.42	54.67	
	layer1	0.07	22.06	37.31	47.91	53.20	55.73	57.26	58.44	59.25	59.13	59.15	58.87	58.43	
8	layer2	0.07	20.54	37.06	46.31	52.09	55.40	57.13	58.63	59.38	59.40	59.39	58.70	58.78	
	layer3	0.05	19.58	35.71	45.55	51.37	54.57	56.81	58.36	59.17	59.42	59.63	59.63	59.67	
	layer4	0.05	19.26	35.43	44.57	50.31	53.40	55.49	57.31	58.53	58.46	58.86	58.77	58.64	
	none	0.00	7.74	19.37	29.25	36.20	41.00	44.29	46.76	48.77	50.13	51.08	52.21	52.53	
	conv0	1.66	21.42	34.27	42.97	46.42	48.64	50.59	51.58	52.05	51.81	49.95	49.89	49.83	
10	layer1	0.00	9.06	20.99	32.37	39.17	43.28	45.92	48.18	50.11	51.32	51.47	52.45	52.38	
	layer2	0.00	8.45	20.75	30.85	38.20	42.80	46.39	48.31	50.16	51.45	51.94	52.66	52.79	
	layer3	0.00	7.88	19.67	29.92	37.09	41.89	45.56	47.98	50.65	50.74	51.99	52.81	53.23	
	layer4	0.00	7.72	19.39	29.29	36.17	41.07	44.30	46.73	49.01	50.12	51.12	52.24	52.47	
	none	0.00	2.66	9.63	17.81	24.41	29.79	33.58	36.81	39.64	41.57	43.21	45.14	45.67	
12	conv0	0.31	10.48	21.49	30.52	35.30	38.55	41.78	43.52	44.50	45.62	44.61	45.06	45.73	
	layer1	0.00	3.01	10.57	20.21	27.04	32.16	35.77	38.30	41.20	43.17	43.86	45.88	46.22	
	layer2	0.00	2.84	10.62	19.09	26.06	31.75	35.77	38.70	41.60	43.13	44.87	46.32	46.69	
	layer3	0.00	2.60	9.60	18.32	25.09	30.91	34.57	38.03	41.04	42.55	44.18	45.98	46.49	
	layer4	0.00	2.68	9.74	17.81	24.47	29.70	33.59	36.70	39.61	41.60	43.17	44.90	45.56	
12	none	0.00	0.94	4.28	9.97	15.48	20.20	24.16	27.80	31.17	33.49	35.74	38.05	39.27	
	conv0	0.11	4.22	12.09	20.08	25.11	28.95	33.79	35.95	37.56	38.69	39.11	40.18	40.98	
	layer1	0.00	1.05	4.94	11.72	17.22	22.47	26.14	29.56	32.69	35.67	36.63	39.61	40.37	
	layer2	0.00	1.01	4.76	11.02	16.84	21.65	26.16	29.72	33.37	35.55	37.93	39.89	40.71	
	layer3	0.00	0.98	4.37	10.32	15.93	21.14	25.26	29.03	32.41	34.70	36.69	38.75	40.29	
layer4	0.00	0.96	4.31	10.06	15.49	20.08	24.20	27.99	31.03	33.60	35.72	38.26	39.32		

Table 9: Evaluation of quantization after four intermediate features of ϵ -robust ResNet-18 models on the Transfer PGD $_{\delta}$ -20 attack at $\beta = 4.0$.

Analysis of Adversarial Training at a Spectrum of Perturbations

δ	Quant. after layer:	ϵ												
		0	1	2	3	4	5	6	7	8	9	10	11	12
2	none	18.15	71.84	77.85	79.01	79.08	78.75	77.77	77.05	76.69	75.57	74.13	72.28	71.01
	conv0	36.49	75.62	79.02	79.35	79.09	78.05	76.25	75.36	74.75	73.37	70.16	68.31	67.53
	layer1	18.75	73.11	78.51	79.60	79.24	79.01	77.94	76.65	76.24	74.51	73.67	71.67	70.01
	layer2	18.70	72.34	78.12	79.18	79.39	78.74	77.92	76.80	76.47	75.62	73.11	71.51	69.74
	layer3	18.27	72.09	77.94	79.11	79.42	78.85	78.06	77.19	76.76	75.81	74.15	72.37	70.93
layer4	18.33	72.04	77.80	78.89	79.16	78.52	77.66	77.01	76.71	75.48	73.75	72.02	70.59	
4	none	1.49	41.50	56.39	62.54	65.46	67.42	67.82	68.16	68.50	67.61	66.88	66.08	65.20
	conv0	8.18	53.08	62.74	67.13	68.15	68.47	68.19	68.22	67.79	66.77	64.62	63.26	62.84
	layer1	1.41	43.82	57.96	64.02	66.30	67.79	68.21	68.29	68.42	67.07	66.84	65.39	64.68
	layer2	1.54	42.46	57.37	63.34	66.30	68.00	68.19	68.40	68.60	67.58	66.67	65.60	64.54
	layer3	1.48	41.67	56.71	63.22	66.06	67.91	68.15	68.58	68.55	68.06	67.26	66.20	65.30
layer4	1.48	41.58	56.53	62.66	65.53	67.24	67.63	67.96	68.18	67.27	66.67	65.77	64.98	
6	none	0.05	19.10	35.31	44.50	50.31	53.50	55.59	57.45	58.60	58.66	59.12	59.03	58.97
	conv0	1.04	29.65	43.82	52.28	55.68	57.51	59.09	59.74	60.09	59.47	58.34	58.25	57.96
	layer1	0.06	20.71	36.63	46.40	52.11	54.85	56.57	58.17	58.95	59.00	58.96	58.96	58.79
	layer2	0.05	19.77	36.20	45.70	51.46	54.58	56.49	58.08	59.08	59.11	59.28	59.32	59.07
	layer3	0.05	19.40	35.49	45.07	50.85	54.23	56.30	58.02	59.01	59.19	59.36	59.44	59.30
layer4	0.05	19.23	35.39	44.47	50.34	53.52	55.58	57.29	58.54	58.32	58.95	58.97	58.66	
8	none	0.00	7.74	19.37	29.25	36.20	41.00	44.29	46.76	48.77	50.13	51.08	52.21	52.53
	conv0	0.06	13.90	27.34	37.94	42.63	45.85	48.71	50.53	51.52	52.12	52.03	52.52	52.52
	layer1	0.00	8.32	20.20	31.05	37.81	42.33	45.34	47.48	49.46	50.89	51.44	52.54	52.41
	layer2	0.00	8.06	20.12	30.04	37.31	42.03	45.49	47.69	49.71	50.70	51.60	52.64	52.63
	layer3	0.00	7.74	19.52	29.51	36.60	41.63	44.91	47.65	49.72	50.60	51.77	52.50	53.08
layer4	0.00	7.72	19.42	29.24	36.24	41.08	44.19	46.77	48.85	50.00	51.10	52.28	52.46	
10	none	0.00	2.66	9.63	17.81	24.41	29.79	33.58	36.81	39.64	41.57	43.21	45.14	45.67
	conv0	0.00	5.64	15.21	24.82	30.62	34.69	39.21	41.33	43.09	44.30	45.63	46.99	46.77
	layer1	0.00	2.81	10.16	19.07	25.93	31.00	34.80	37.54	40.52	42.41	43.59	45.59	46.04
	layer2	0.00	2.79	10.11	18.58	25.48	30.91	34.94	38.00	40.71	42.45	44.21	45.92	46.27
	layer3	0.00	2.65	9.51	18.07	24.66	30.46	34.19	37.49	40.46	42.09	43.80	45.63	45.96
layer4	0.00	2.68	9.71	17.77	24.38	29.75	33.54	36.75	39.74	41.51	43.18	45.20	45.56	
12	none	0.00	0.94	4.28	9.97	15.48	20.20	24.16	27.80	31.17	33.49	35.74	38.05	39.27
	conv0	0.00	2.06	7.77	14.94	20.27	25.07	30.02	32.71	34.89	36.89	38.86	40.64	41.23
	layer1	0.00	1.00	4.54	10.94	16.35	21.47	25.28	28.82	31.99	34.78	36.22	39.06	39.88
	layer2	0.00	1.00	4.55	10.65	16.31	21.01	25.36	28.83	32.45	34.71	37.02	39.40	40.21
	layer3	0.00	0.95	4.28	10.17	15.62	20.62	24.84	28.44	31.97	34.32	36.45	38.51	39.87
layer4	0.00	0.95	4.31	10.04	15.46	20.17	24.20	27.94	31.07	33.65	35.91	38.08	39.06	

Table 10: Evaluation of quantization after four intermediate features of ϵ -robust ResNet-18 models on the Transfer PGD $_{\delta}$ -20 attack at $\beta = 6.0$.

δ	Quant. after layer:	ϵ												
		0	1	2	3	4	5	6	7	8	9	10	11	12
2	none	18.15	71.84	77.85	79.01	79.08	78.75	77.77	77.05	76.69	75.57	74.13	72.28	71.01
	conv0	28.66	74.58	78.99	79.55	79.65	78.98	77.49	76.61	76.26	74.94	72.81	71.17	69.93
	layer1	18.42	72.62	78.24	79.38	79.36	78.92	77.83	76.86	76.52	75.05	73.77	71.90	70.51
	layer2	18.52	72.26	78.02	79.01	79.22	78.87	77.96	76.90	76.73	75.56	73.77	71.85	70.42
	layer3	18.27	72.21	77.83	79.06	79.34	78.83	77.91	77.22	76.61	75.97	74.22	72.47	71.12
layer4	18.36	72.00	77.89	79.00	79.15	78.62	77.65	77.02	76.73	75.52	73.96	72.08	70.66	
4	none	1.49	41.50	56.39	62.54	65.46	67.42	67.82	68.16	68.50	67.61	66.88	66.08	65.20
	conv0	3.29	47.89	60.51	65.48	67.30	68.26	68.43	68.55	68.57	67.59	66.24	65.22	64.42
	layer1	1.43	42.43	57.25	63.31	66.00	67.64	68.00	68.24	68.31	67.42	66.75	65.83	65.05
	layer2	1.52	42.08	56.94	63.07	65.87	67.82	68.03	68.26	68.33	67.62	66.80	65.73	65.01
	layer3	1.46	41.67	56.74	62.72	65.75	67.77	67.97	68.67	68.60	67.89	67.21	66.21	65.27
layer4	1.50	41.63	56.48	62.67	65.47	67.37	67.66	68.08	68.32	67.50	66.72	65.97	65.23	
6	none	0.05	19.10	35.31	44.50	50.31	53.50	55.59	57.45	58.60	58.66	59.12	59.03	58.97
	conv0	0.16	24.43	39.76	48.96	53.64	55.95	57.96	58.94	59.74	59.56	59.10	59.27	58.84
	layer1	0.05	19.83	35.94	45.55	51.20	54.14	56.01	57.75	58.79	58.79	58.99	59.08	59.00
	layer2	0.05	19.53	35.79	45.11	50.76	53.97	55.95	57.83	58.68	58.87	59.17	59.27	59.07
	layer3	0.05	19.19	35.40	44.83	50.56	53.98	56.09	57.73	58.81	58.92	59.28	59.16	59.33
layer4	0.05	19.16	35.29	44.48	50.32	53.45	55.59	57.39	58.62	58.54	58.96	58.84	58.84	
8	none	0.00	7.74	19.37	29.25	36.20	41.00	44.29	46.76	48.77	50.13	51.08	52.21	52.53
	conv0	0.00	10.37	23.46	33.43	39.70	43.41	46.91	48.88	50.43	51.26	52.40	53.06	52.75
	layer1	0.00	7.97	19.68	30.16	37.01	41.67	44.78	47.12	49.28	50.58	51.23	52.42	52.42
	layer2	0.00	7.88	19.71	29.56	36.74	41.70	44.90	47.24	49.36	50.53	51.43	52.38	52.81
	layer3	0.00	7.67	19.43	29.37	36.28	41.47	44.48	47.25	49.37	50.29	51.35	52.51	52.71
layer4	0.00	7.69	19.34	29.20	36.20	41.08	44.26	46.84	48.79	50.09	51.10	52.19	52.55	
10	none	0.00	2.66	9.63	17.81	24.41	29.79	33.58	36.81	39.64	41.57	43.21	45.14	45.67
	conv0	0.00	3.69	12.20	20.99	27.50	32.11	36.55	39.04	41.56	43.31	44.84	46.54	46.76
	layer1	0.00	2.68	9.93	18.50	25.19	30.46	34.25	37.10	40.02	41.78	43.43	45.43	45.82
	layer2	0.00	2.71	9.82	18.17	24.75	30.39	34.36	37.31	40.30	42.09	43.87	45.64	45.84
	layer3	0.00	2.63	9.59	17.93	24.57	30.17	33.73	37.25	40.09	41.77	43.63	45.55	45.93
layer4	0.00	2.66	9.69	17.80	24.43	29.71	33.60	36.71	39.66	41.54	43.28	45.17	45.55	
12	none	0.00	0.94	4.28	9.97	15.48	20.20	24.16	27.80	31.17	33.49	35.74	38.05	39.27
	conv0	0.00	1.36	5.93	12.21	17.77	22.64	26.87	29.78	32.87	35.31	37.45	39.52	40.46
	layer1	0.00	0.98	4.44	10.38	15.86	20.87	24.77	28.27	31.64	34.33	36.00	38.52	39.47
	layer2	0.00	0.96	4.43	10.22	15.95	20.53	24.84	28.36	31.85	34.32	36.48	38.79	39.80
	layer3	0.00	0.93	4.30	10.03	15.63	20.34	24.58	28.10	31.69	33.93	36.15	38.50	39.25
layer4	0.00	0.95	4.30	9.99	15.44	20.23	24.20	27.90	31.16	33.44	35.91	38.11	38.95	

Table 11: Evaluation of quantization after four intermediate features of ϵ -robust ResNet-18 models on the Transfer PGD $_{\delta}$ -20 attack at $\beta = 10.0$.

Analysis of Adversarial Training at a Spectrum of Perturbations

δ	Quant. after layer:	ϵ												
		0	1	2	3	4	5	6	7	8	9	10	11	12
2	none	18.15	71.84	77.85	79.01	79.08	78.75	77.77	77.05	76.69	75.57	74.13	72.28	71.01
	conv0	26.63	74.31	78.74	79.42	79.62	79.00	77.75	76.70	76.40	75.16	73.27	71.85	70.34
	layer1	18.34	72.53	78.21	79.29	79.21	78.90	77.89	76.87	76.63	75.24	73.98	71.88	70.71
	layer2	18.44	72.22	77.88	79.15	79.22	78.84	77.91	76.84	76.76	75.55	73.85	71.98	70.55
	layer3	18.32	72.12	77.96	79.03	79.22	78.83	77.92	77.20	76.71	75.86	74.19	72.47	71.10
4	layer4	18.39	71.98	77.86	78.98	79.14	78.64	77.72	77.07	76.69	75.60	74.07	72.15	70.69
	none	1.49	41.50	56.39	62.54	65.46	67.42	67.82	68.16	68.50	67.61	66.88	66.08	65.20
	conv0	2.72	46.53	59.75	64.90	67.06	68.18	68.35	68.49	68.74	67.71	66.45	65.56	64.78
	layer1	1.43	42.21	57.19	63.21	65.80	67.67	67.89	68.22	68.37	67.52	66.77	65.88	65.03
	layer2	1.53	41.99	56.89	62.95	65.76	67.78	67.96	68.22	68.42	67.62	66.68	65.86	64.92
6	layer3	1.46	41.44	56.68	62.75	65.70	67.60	67.93	68.39	68.67	67.77	67.11	66.19	65.35
	layer4	1.50	41.57	56.47	62.63	65.52	67.36	67.72	68.03	68.27	67.46	66.74	65.92	65.20
	none	0.05	19.10	35.31	44.50	50.31	53.50	55.59	57.45	58.60	58.66	59.12	59.03	58.97
	conv0	0.13	23.23	38.93	47.84	52.99	55.47	57.49	58.75	59.62	59.36	59.08	59.29	58.93
	layer1	0.05	19.69	35.70	45.32	51.09	53.99	55.95	57.65	58.69	58.70	58.97	59.09	58.96
8	layer2	0.05	19.43	35.75	45.02	50.63	53.79	55.86	57.67	58.61	58.88	59.22	59.16	59.09
	layer3	0.05	19.17	35.39	44.67	50.55	53.86	56.08	57.62	58.75	58.71	59.21	59.21	59.25
	layer4	0.05	19.13	35.26	44.53	50.37	53.42	55.51	57.42	58.64	58.61	58.94	58.89	58.91
	none	0.00	7.74	19.37	29.25	36.20	41.00	44.29	46.76	48.77	50.13	51.08	52.21	52.53
	conv0	0.00	9.76	22.43	32.50	38.89	43.00	46.38	48.43	50.11	51.17	52.19	53.02	52.76
10	layer1	0.00	7.89	19.61	29.85	36.87	41.55	44.74	47.02	49.25	50.48	51.15	52.43	52.40
	layer2	0.00	7.82	19.61	29.48	36.58	41.43	44.72	47.18	49.33	50.43	51.29	52.21	52.67
	layer3	0.00	7.66	19.40	29.24	36.29	41.32	44.60	47.09	49.24	50.26	51.36	52.40	52.71
	layer4	0.00	7.70	19.35	29.21	36.18	41.03	44.11	46.86	48.76	50.07	50.95	52.23	52.52
	none	0.00	2.66	9.63	17.81	24.41	29.79	33.58	36.81	39.64	41.57	43.21	45.14	45.67
12	conv0	0.00	3.32	11.74	20.22	26.84	31.74	35.95	38.61	41.14	42.86	44.47	46.17	46.42
	layer1	0.00	2.65	9.85	18.32	24.93	30.25	34.16	36.95	39.99	41.76	43.39	45.35	45.68
	layer2	0.00	2.68	9.79	18.11	24.63	30.30	34.22	37.24	40.20	41.94	43.80	45.54	45.79
	layer3	0.00	2.63	9.53	17.82	24.48	29.97	33.78	37.13	39.96	41.73	43.48	45.40	45.91
	layer4	0.00	2.69	9.69	17.83	24.40	29.72	33.58	36.69	39.81	41.52	43.21	45.16	45.60
12	none	0.00	0.94	4.28	9.97	15.48	20.20	24.16	27.80	31.17	33.49	35.74	38.05	39.27
	conv0	0.00	1.30	5.61	11.69	17.15	22.15	26.27	29.40	32.41	35.07	37.07	39.30	40.35
	layer1	0.00	0.98	4.37	10.29	15.82	20.72	24.63	28.23	31.58	34.20	36.04	38.39	39.42
	layer2	0.00	0.96	4.39	10.15	15.80	20.45	24.72	28.23	31.68	34.08	36.38	38.77	39.62
	layer3	0.00	0.95	4.27	10.01	15.55	20.26	24.58	27.94	31.58	33.79	36.01	38.43	39.24
layer4	0.00	0.94	4.27	9.99	15.41	20.22	24.15	27.89	31.09	33.52	35.84	38.01	39.03	

Table 12: Evaluation of quantization after four intermediate features of ϵ -robust ResNet-18 models on the Transfer PGD $_{\delta}$ -20 attack at $\beta = 12.0$.

δ	Quant. after layer:	ϵ							
		0	2	4	6	8	10	12	
2	none	2.43	81.77	82.67	81.58	79.19	76.23	71.20	
	init conv	2.35	81.63	82.76	81.60	79.06	75.95	70.90	
	layer[0]	2.29	81.85	82.60	81.42	78.92	76.05	70.92	
	layer[1]	2.40	81.72	82.76	81.54	79.01	75.99	70.46	
	layer[2]	2.47	81.68	82.74	81.45	79.00	75.98	70.78	
4	none	0.00	62.12	70.87	72.80	71.81	69.95	66.20	
	init conv	0.00	61.86	70.83	72.93	71.53	69.62	65.87	
	layer[0]	0.00	62.43	70.90	73.06	71.78	69.79	65.97	
	layer[1]	0.00	62.12	70.92	72.86	71.74	69.75	65.82	
	layer[2]	0.00	62.15	70.90	72.74	71.77	69.91	65.70	
6	none	0.00	39.50	56.25	62.01	62.91	63.28	60.54	
	init conv	0.00	39.40	56.28	62.11	62.92	63.02	60.61	
	layer[0]	0.00	40.42	56.73	62.10	62.88	63.08	60.48	
	layer[1]	0.00	39.75	56.42	62.31	62.96	63.27	60.26	
	layer[2]	0.00	39.54	56.26	62.13	62.94	63.17	60.45	
8	none	0.00	22.08	41.20	49.83	53.72	55.81	54.67	
	init conv	0.00	21.88	41.26	49.78	53.80	55.55	54.34	
	layer[0]	0.00	22.75	41.74	49.92	53.92	55.64	54.42	
	layer[1]	0.00	22.24	41.39	50.08	53.94	55.58	54.49	
	layer[2]	0.00	22.01	41.21	49.84	53.77	55.53	54.62	
10	none	0.00	11.15	28.19	38.37	44.65	47.70	48.12	
	init conv	0.00	10.89	28.28	38.35	44.58	47.78	48.34	
	layer[0]	0.00	11.69	28.84	38.85	45.02	47.92	48.45	
	layer[1]	0.00	11.23	28.47	38.79	44.82	47.68	48.66	
	layer[2]	0.00	11.15	28.34	38.57	44.61	47.66	48.20	
12	none	0.00	5.18	17.54	28.08	35.93	39.84	42.09	
	init conv	0.00	5.08	17.62	28.12	35.79	39.72	42.06	
	layer[0]	0.00	5.35	18.19	28.61	36.18	39.92	42.21	
	layer[1]	0.00	5.25	17.85	28.27	36.34	40.32	42.38	
	layer[2]	0.00	5.15	17.63	28.22	36.22	40.04	42.26	

Table 13: Evaluation of quantization after four intermediate features of ϵ -robust WideResNet-28-10 models on the Transfer PGD $_{\delta}$ -20 attack for various ϵ and δ at $\beta = 8.0$.

Analysis of Adversarial Training at a Spectrum of Perturbations

δ	Quant. after layer:	ϵ						
		0	2	4	6	8	10	12
2	none	2.43	81.77	82.67	81.58	79.19	76.23	71.20
	init conv	2.45	81.65	82.69	81.60	78.93	75.53	70.61
	layer[0]	2.19	82.02	82.60	81.23	78.52	76.08	70.52
	layer[1]	2.41	81.72	82.80	81.33	78.68	75.66	69.62
	layer[2]	2.51	81.65	82.67	81.22	78.64	75.63	70.19
4	none	0.00	62.12	70.87	72.80	71.81	69.95	66.20
	init conv	0.00	61.71	70.87	72.88	71.41	69.44	65.58
	layer[0]	0.00	62.84	71.13	73.02	71.53	69.43	65.41
	layer[1]	0.00	62.24	71.05	72.77	71.60	69.64	65.15
	layer[2]	0.00	62.19	70.96	72.59	71.52	69.37	65.09
6	none	0.00	39.50	56.25	62.01	62.91	63.28	60.54
	init conv	0.00	39.36	56.37	62.07	62.96	62.53	60.03
	layer[0]	0.00	41.29	57.01	62.28	62.92	62.81	60.19
	layer[1]	0.00	40.01	56.61	62.38	63.15	63.23	59.72
	layer[2]	0.00	39.63	56.31	62.28	62.92	62.78	60.27
8	none	0.00	22.08	41.20	49.83	53.72	55.81	54.67
	init conv	0.00	21.56	41.24	49.62	53.66	55.57	54.22
	layer[0]	0.00	23.54	42.15	50.54	54.22	55.65	54.31
	layer[1]	0.00	22.39	41.50	50.25	54.07	55.59	54.49
	layer[2]	0.00	22.03	41.39	49.92	54.10	55.53	54.53
10	none	0.00	11.15	28.19	38.37	44.65	47.70	48.12
	init conv	0.00	10.93	28.35	38.33	44.41	47.78	48.38
	layer[0]	0.00	12.25	29.43	39.32	45.18	48.11	48.46
	layer[1]	0.00	11.38	28.69	39.04	45.08	47.97	48.41
	layer[2]	0.00	11.13	28.43	38.85	44.60	47.87	48.38
12	none	0.00	5.18	17.54	28.08	35.93	39.84	42.09
	init conv	0.00	5.05	17.79	28.23	35.65	39.95	41.86
	layer[0]	0.00	5.71	19.10	29.30	36.61	40.34	42.21
	layer[1]	0.00	5.32	18.23	28.65	36.55	40.72	42.31
	layer[2]	0.00	5.16	17.75	28.42	36.29	40.16	42.14

Table 14: Evaluation of quantization after four intermediate features of ϵ -robust WideResNet-28-10 models on the Transfer PGD $_{\delta}$ -20 attack at $\beta = 4.0$.

δ	Quant. after layer:	ϵ						
		0	2	4	6	8	10	12
2	none	2.43	81.77	82.67	81.58	79.19	76.23	71.20
	init conv	2.37	81.63	82.82	81.55	79.12	75.80	70.85
	layer[0]	2.26	81.90	82.55	81.39	78.75	76.10	70.89
	layer[1]	2.40	81.69	82.75	81.44	78.86	75.97	70.21
	layer[2]	2.50	81.68	82.75	81.40	78.96	75.82	70.55
4	none	0.00	62.12	70.87	72.80	71.81	69.95	66.20
	init conv	0.00	61.68	70.77	72.92	71.42	69.62	65.79
	layer[0]	0.00	62.64	70.88	73.08	71.59	69.75	65.75
	layer[1]	0.00	62.22	70.94	72.84	71.72	69.68	65.60
	layer[2]	0.00	62.19	70.94	72.69	71.66	69.70	65.51
6	none	0.00	39.50	56.25	62.01	62.91	63.28	60.54
	init conv	0.00	39.41	56.25	62.09	62.90	62.88	60.39
	layer[0]	0.00	40.59	56.88	62.16	62.85	63.00	60.38
	layer[1]	0.00	39.80	56.54	62.35	62.92	63.23	60.06
	layer[2]	0.00	39.55	56.32	62.17	62.95	63.13	60.55
8	none	0.00	22.08	41.20	49.83	53.72	55.81	54.67
	init conv	0.00	21.70	41.24	49.71	53.77	55.50	54.28
	layer[0]	0.00	22.99	41.85	50.17	53.98	55.61	54.47
	layer[1]	0.00	22.29	41.50	50.14	54.09	55.68	54.55
	layer[2]	0.00	22.01	41.36	49.81	53.97	55.43	54.62
10	none	0.00	11.15	28.19	38.37	44.65	47.70	48.12
	init conv	0.00	10.92	28.30	38.36	44.56	47.79	48.37
	layer[0]	0.00	11.86	29.07	38.98	45.00	47.91	48.53
	layer[1]	0.00	11.26	28.52	38.93	44.92	47.88	48.54
	layer[2]	0.00	11.13	28.30	38.62	44.63	47.72	48.34
12	none	0.00	5.18	17.54	28.08	35.93	39.84	42.09
	init conv	0.00	5.08	17.69	28.13	35.68	39.76	41.97
	layer[0]	0.00	5.49	18.54	28.76	36.34	39.93	42.08
	layer[1]	0.00	5.24	17.95	28.30	36.34	40.45	42.35
	layer[2]	0.00	5.15	17.65	28.31	36.27	40.08	42.19

Table 15: Evaluation of quantization after four intermediate features of ϵ -robust WideResNet-28-10 models on the Transfer PGD $_{\delta}$ -20 attack at $\beta = 6.0$.

δ	Quant. after layer:	ϵ						
		0	2	4	6	8	10	12
2	none	2.43	81.77	82.67	81.58	79.19	76.23	71.20
	init conv	2.39	81.61	82.74	81.59	79.20	76.04	71.04
	layer[0]	2.31	81.80	82.66	81.46	78.92	76.10	71.12
	layer[1]	2.42	81.75	82.74	81.57	79.11	76.07	70.70
	layer[2]	2.45	81.72	82.73	81.43	79.02	76.06	70.86
4	none	0.00	62.12	70.87	72.80	71.81	69.95	66.20
	init conv	0.00	61.86	70.81	72.95	71.58	69.60	65.96
	layer[0]	0.00	62.34	70.96	73.00	71.85	69.78	66.03
	layer[1]	0.00	62.15	70.91	72.88	71.79	69.88	65.91
	layer[2]	0.00	62.14	70.90	72.74	71.77	69.93	65.89
6	none	0.00	39.50	56.25	62.01	62.91	63.28	60.54
	init conv	0.00	39.37	56.22	62.10	62.94	63.03	60.59
	layer[0]	0.00	40.20	56.63	62.12	62.91	63.10	60.50
	layer[1]	0.00	39.63	56.35	62.24	63.01	63.32	60.41
	layer[2]	0.00	39.54	56.26	62.19	62.98	63.17	60.50
8	none	0.00	22.08	41.20	49.83	53.72	55.81	54.67
	init conv	0.00	21.88	41.14	49.77	53.71	55.65	54.39
	layer[0]	0.00	22.57	41.56	49.84	53.94	55.58	54.45
	layer[1]	0.00	22.13	41.37	50.00	53.93	55.56	54.54
	layer[2]	0.00	22.02	41.20	49.80	53.72	55.60	54.55
10	none	0.00	11.15	28.19	38.37	44.65	47.70	48.12
	init conv	0.00	10.94	28.26	38.36	44.71	47.79	48.29
	layer[0]	0.00	11.52	28.73	38.78	44.97	47.85	48.43
	layer[1]	0.00	11.19	28.42	38.69	44.85	47.70	48.47
	layer[2]	0.00	11.15	28.29	38.48	44.61	47.68	48.26
12	none	0.00	5.18	17.54	28.08	35.93	39.84	42.09
	init conv	0.00	5.05	17.56	28.14	35.77	39.73	42.12
	layer[0]	0.00	5.29	18.12	28.51	36.01	39.94	42.20
	layer[1]	0.00	5.23	17.78	28.23	36.21	40.24	42.31
	layer[2]	0.00	5.15	17.58	28.19	36.09	40.03	42.21

Table 16: Evaluation of quantization after four intermediate features of ϵ -robust WideResNet-28-10 models on the Transfer PGD $_{\delta}$ -20 attack at $\beta = 10.0$.

δ	Quant. after layer:	ϵ						
		0	2	4	6	8	10	12
2	none	2.43	81.77	82.67	81.58	79.19	76.23	71.20
	init conv	2.37	81.64	82.78	81.60	79.24	76.02	71.06
	layer[0]	2.36	81.84	82.66	81.46	78.95	76.02	71.20
	layer[1]	2.43	81.80	82.71	81.58	79.14	76.05	70.83
	layer[2]	2.44	81.73	82.76	81.44	79.09	76.03	70.98
4	none	0.00	62.12	70.87	72.80	71.81	69.95	66.20
	init conv	0.00	61.83	70.85	72.83	71.63	69.71	65.99
	layer[0]	0.00	62.27	70.94	73.01	71.80	69.81	66.01
	layer[1]	0.00	62.23	70.89	72.87	71.75	69.92	65.96
	layer[2]	0.00	62.12	70.86	72.76	71.78	69.87	65.90
6	none	0.00	39.50	56.25	62.01	62.91	63.28	60.54
	init conv	0.00	39.42	56.24	62.14	62.94	63.18	60.69
	layer[0]	0.00	40.02	56.49	62.01	62.90	63.06	60.51
	layer[1]	0.00	39.59	56.34	62.22	62.99	63.27	60.53
	layer[2]	0.00	39.51	56.29	62.14	62.95	63.22	60.48
8	none	0.00	22.08	41.20	49.83	53.72	55.81	54.67
	init conv	0.00	21.92	41.12	49.69	53.77	55.68	54.39
	layer[0]	0.00	22.48	41.48	49.79	53.87	55.52	54.60
	layer[1]	0.00	22.05	41.35	50.01	53.94	55.62	54.57
	layer[2]	0.00	22.01	41.22	49.77	53.75	55.62	54.59
10	none	0.00	11.15	28.19	38.37	44.65	47.70	48.12
	init conv	0.00	10.94	28.24	38.36	44.64	47.76	48.31
	layer[0]	0.00	11.46	28.63	38.71	44.99	47.75	48.35
	layer[1]	0.00	11.15	28.37	38.60	44.85	47.62	48.40
	layer[2]	0.00	11.11	28.28	38.44	44.64	47.66	48.37
12	none	0.00	5.18	17.54	28.08	35.93	39.84	42.09
	init conv	0.00	5.12	17.58	28.11	35.84	39.74	42.06
	layer[0]	0.00	5.25	18.03	28.43	36.05	39.91	42.15
	layer[1]	0.00	5.20	17.70	28.21	36.20	40.16	42.25
	layer[2]	0.00	5.13	17.58	28.18	36.03	40.06	42.27

Table 17: Evaluation of quantization after four intermediate features of ϵ -robust WideResNet-28-10 models on the Transfer PGD $_{\delta}$ -20 attack at $\beta = 12.0$.

C.3. Clean Accuracies After Quantization for Various β

Analysis of Adversarial Training at a Spectrum of Perturbations

β	Quant. after layer:	ϵ												
		0	1	2	3	4	5	6	7	8	9	10	11	12
4	none	85.58	92.25	91.79	90.16	89.09	87.95	86.35	84.66	83.63	82.23	80.32	78.33	76.50
	conv0	65.40	85.60	86.70	85.00	84.00	82.30	85.00	82.70	81.00	79.10	77.80	75.00	73.50
	layer1	84.50	91.50	91.40	89.00	88.00	86.00	85.20	83.50	82.00	79.90	78.70	75.90	73.80
	layer2	84.50	91.00	91.30	89.90	88.70	87.20	85.40	83.60	82.20	81.20	77.60	75.80	73.60
	layer3	85.30	92.00	91.30	89.80	88.60	87.00	86.30	84.50	83.10	81.90	79.00	78.00	75.90
6	layer4	85.30	92.30	91.70	90.10	89.00	87.00	86.20	84.00	83.20	81.70	79.90	77.40	75.40
	none	85.58	92.25	91.79	90.16	89.09	87.95	86.35	84.66	83.63	82.23	80.32	78.33	76.50
	conv0	75.40	90.30	89.70	88.00	86.80	85.10	82.70	81.60	80.00	78.70	75.50	73.10	72.00
	layer1	84.90	92.10	91.70	89.80	88.50	87.20	85.90	84.10	83.00	81.00	79.40	76.80	75.20
	layer2	84.90	92.10	91.50	90.10	88.70	87.00	85.90	84.00	82.70	81.70	78.90	77.00	75.10
8	layer3	85.50	92.20	91.60	89.80	88.90	88.00	86.40	84.60	83.20	82.00	79.90	78.20	76.20
	layer4	85.40	92.20	91.70	90.10	89.10	87.80	86.30	84.00	83.30	82.00	80.00	77.80	76.00
	none	85.58	92.25	91.79	90.16	89.09	87.95	86.35	84.66	83.63	82.23	80.32	78.33	76.50
	conv0	79.90	91.30	90.70	88.70	87.70	86.20	84.40	82.60	82.00	80.00	77.50	75.70	73.60
	layer1	85.10	92.00	91.70	89.80	88.60	87.40	86.00	84.40	83.20	81.40	79.70	77.20	75.60
10	layer2	85.10	92.20	91.50	90.10	88.80	87.80	85.90	84.30	83.00	81.70	79.40	77.40	75.40
	layer3	85.50	92.20	91.70	90.00	89.00	87.90	86.50	84.70	83.40	82.10	80.00	78.30	76.20
	layer4	85.40	92.20	91.70	90.10	89.10	87.90	86.40	84.50	83.40	82.00	80.10	78.00	76.10
	none	85.58	92.25	91.79	90.16	89.09	87.95	86.35	84.66	83.63	82.23	80.32	78.33	76.50
	conv0	81.40	91.00	91.10	89.20	88.10	86.00	85.10	83.30	82.30	80.00	78.30	76.50	74.50
12	layer1	85.20	92.30	91.70	89.00	88.70	87.50	86.00	84.40	83.00	81.60	79.80	77.40	75.90
	layer2	85.20	92.20	91.70	90.00	88.90	87.70	86.00	84.40	83.20	81.80	79.00	77.50	75.00
	layer3	85.00	92.20	91.70	90.00	89.00	87.90	86.50	84.70	83.00	82.20	80.20	78.20	76.30
	layer4	85.40	92.20	91.70	90.10	89.10	87.90	86.40	84.60	83.40	82.00	80.20	78.00	76.00
	none	85.58	92.25	91.79	90.16	89.09	87.95	86.35	84.66	83.63	82.23	80.32	78.33	76.50
12	conv0	82.60	91.90	91.00	89.40	88.50	86.90	85.20	83.60	82.50	81.00	78.00	76.80	74.90
	layer1	85.30	92.20	91.70	89.90	88.80	87.00	86.20	84.50	83.20	81.70	79.90	77.60	76.00
	layer2	85.20	92.20	91.70	90.20	88.90	87.80	86.10	84.50	83.30	81.90	79.70	77.70	75.80
	layer3	85.50	92.20	91.80	90.00	89.00	87.90	86.60	84.70	83.50	82.30	80.10	78.30	76.00
	layer4	85.40	92.20	91.70	90.10	89.10	87.90	86.30	84.60	83.00	82.00	80.20	78.10	76.30

Table 18: Clean accuracy evaluation of quantization at various $\beta \in \{4, 6, 8, 10, 12\}$ after four intermediate features of ϵ -robust ResNet18 models.

β	Quant. after layer:	ϵ						
		0	2	4	6	8	10	12
4	none	85.45	93.41	91.13	88.66	85.23	81.51	75.83
	init conv	84.00	93.30	90.90	88.30	84.80	81.00	75.50
	layer[0]	85.60	93.10	90.90	88.10	84.60	81.30	75.10
	layer[1]	85.10	93.30	91.00	88.40	84.80	80.70	74.30
	layer[2]	85.10	93.30	91.10	88.40	84.70	80.70	74.80
6	none	85.45	93.41	91.13	88.66	85.23	81.51	75.83
	init conv	84.90	93.30	91.00	88.40	85.00	81.30	75.70
	layer[0]	85.70	93.20	91.00	88.30	85.00	81.60	75.50
	layer[1]	85.30	93.50	91.00	88.50	84.90	80.90	75.00
	layer[2]	85.10	93.30	91.10	88.50	84.90	81.00	75.10
8	none	85.45	93.41	91.13	88.66	85.23	81.51	75.83
	init conv	84.90	93.30	91.00	88.40	85.20	81.40	75.80
	layer[0]	85.60	93.30	91.00	88.40	85.10	81.50	75.60
	layer[1]	85.40	93.00	91.00	88.60	85.00	81.00	75.20
	layer[2]	85.10	93.30	91.20	88.50	85.00	81.20	75.30
10	none	85.45	93.41	91.13	88.66	85.23	81.51	75.83
	init conv	85.20	93.30	91.00	88.50	85.10	81.30	75.80
	layer[0]	85.50	93.30	91.00	88.40	85.10	81.50	75.70
	layer[1]	85.00	93.40	91.00	88.60	85.10	81.20	75.30
	layer[2]	85.20	93.30	91.10	88.50	85.10	81.30	75.40
12	none	85.45	93.41	91.13	88.66	85.23	81.51	75.83
	init conv	85.20	93.30	91.00	88.50	85.20	81.30	75.80
	layer[0]	85.50	93.40	91.00	88.00	85.10	81.50	75.70
	layer[1]	85.40	93.40	91.00	88.00	85.10	81.30	75.30
	layer[2]	85.30	93.30	91.20	88.60	85.10	81.30	75.50

Table 19: Clean accuracy evaluation of quantization at various $\beta \in \{4, 6, 8, 10, 12\}$ after four intermediate features of ϵ -robust WideResNet-28-10 models.

D. AT and Norm of CNN Kernels

We analyze the worst case performance by plotting (for convolution layer i), $\max_{w \in \text{conv } i} \|w\|_\infty$ for various layers of increasing ϵ -robust models in Figure 5. We note a large separation between the first two layers and other layers (as previously observed in the average case in Section 5) but also observe a monotonic increase for the first two curves of ResNet18 but not WideResNet-28-10.

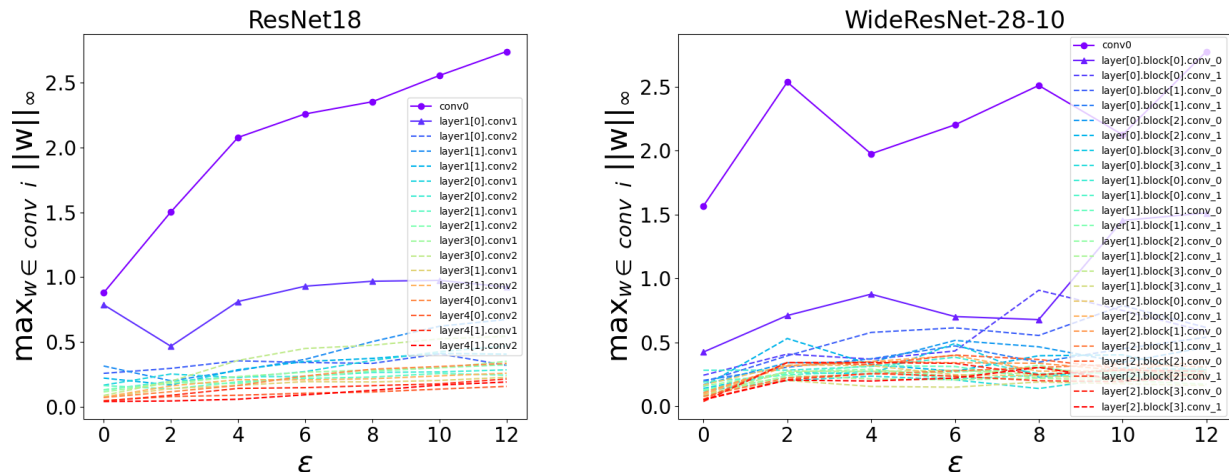


Figure 5: Plot of maximum of L_∞ norms of filters in various layers for increasingly ϵ -robust ResNet18 (left) and WideResNet-28-10 (right) models.

E. Training with Larger Perturbations and Common-Corruptions

We present the accuracy of non-robust and various ϵ -robust models for each corruption with ResNet18 models, and WideResNet-18 models in Tables 20, and 21 respectively.

corruption	non-robust	1	2	3	4	5	6	7	8	9	10	11	12
gaussian noise	51.33	80.59	<u>84.09</u>	84.59	83.75	82.65	81.63	80.28	79.34	78.25	76.66	74.49	73.2
shot noise	60.0	84.34	86.06	85.92	84.91	83.63	82.56	81.06	80.19	78.93	77.45	75.23	73.82
impulse noise	55.82	68.8	73.3	76.08	75.34	<u>75.94</u>	74.58	74.08	73.7	73.61	72.97	71.26	70.59
defocus blur	71.58	<u>84.64</u>	85.02	84.47	83.62	82.74	81.61	80.01	79.27	77.86	76.39	74.43	72.94
glass blur	46.46	75.54	79.53	80.4	80.51	80.21	79.58	78.37	77.54	76.5	74.83	72.86	71.52
motion blur	61.78	79.65	<u>79.89</u>	80.32	79.1	78.71	77.6	76.13	75.61	74.3	72.58	71.22	69.85
zoom blur	68.7	<u>83.51</u>	83.73	83.42	82.36	81.68	80.82	79.35	78.58	77.08	75.57	73.98	72.43
snow	68.29	<u>84.94</u>	85.02	83.68	82.87	81.52	80.31	78.96	77.9	76.26	75.11	72.95	71.35
frost	67.53	85.79	<u>84.86</u>	82.66	80.85	78.8	76.96	74.93	73.19	70.98	69.1	66.9	64.67
fog	<u>73.15</u>	75.59	70.56	67.13	65.01	62.91	61.2	59.29	58.49	57.12	55.44	54.54	53.14
brightness	81.99	90.62	<u>89.63</u>	87.53	86.17	84.33	82.73	81.21	80.03	78.05	76.5	74.47	72.63
contrast	<u>57.68</u>	59.15	53.91	51.19	48.77	46.44	45.02	43.04	42.46	41.43	40.42	40.08	39.23
elastic transform	73.0	85.19	<u>84.86</u>	84.0	82.94	81.88	80.72	79.24	78.29	76.8	74.92	73.23	71.56
pixelate	65.45	<u>88.42</u>	88.88	87.81	86.89	85.79	84.36	82.64	81.7	80.3	78.62	76.49	74.92
jpeg compression	72.0	<u>88.94</u>	89.13	87.99	86.73	85.7	84.33	82.58	81.79	80.44	78.59	76.47	75.14
speckle noise	61.67	83.76	<u>85.45</u>	85.55	84.63	83.38	81.98	80.8	79.92	78.73	77.28	74.95	73.6
gaussian blur	65.23	80.94	<u>81.75</u>	81.94	81.08	80.51	79.38	77.93	77.16	75.99	74.46	72.73	71.39
spatter	73.13	85.72	<u>85.25</u>	84.29	83.59	82.42	81.34	80.2	79.16	78.0	76.31	74.54	73.06
saturate	79.28	88.04	<u>86.59</u>	85.38	84.42	83.06	82.04	80.27	79.49	78.07	76.52	74.68	72.89
Avg.	66.0	<u>81.8</u>	81.97	81.28	80.19	79.07	77.83	76.33	75.46	74.14	72.62	70.82	69.37

Table 20: Accuracy of ϵ -robust models (from $\epsilon = 1$ to 12) on various common corruptions. The bold and underlined values denote the largest and second largest value in each row (*i.e.*, for each type of corruption).

Analysis of Adversarial Training at a Spectrum of Perturbations

corruption	non-robust	2	4	6	8	10	12
gaussian noise	28.42	<u>85.44</u>	86.26	83.55	80.59	77.55	72.5
shot noise	38.11	87.43	<u>87.29</u>	84.8	81.71	78.4	73.33
impulse noise	48.51	74.52	78.34	<u>77.15</u>	75.37	74.28	71.29
defocus blur	67.26	86.73	<u>85.1</u>	83.0	80.14	76.93	71.49
glass blur	34.11	79.06	81.64	<u>80.07</u>	77.81	74.97	69.8
motion blur	59.05	81.83	<u>80.76</u>	78.73	75.93	73.09	68.42
zoom blur	58.12	85.6	<u>83.69</u>	82.04	79.0	75.9	70.56
snow	62.43	87.52	<u>86.19</u>	83.11	79.98	76.56	70.91
frost	56.36	87.34	<u>84.79</u>	80.14	75.9	70.26	63.72
fog	<u>72.36</u>	74.35	67.98	62.79	59.07	56.41	52.5
brightness	83.06	91.84	<u>89.38</u>	85.76	82.05	78.23	71.71
contrast	<u>55.34</u>	58.58	50.42	45.36	41.95	40.42	38.19
elastic transform	67.85	86.52	<u>84.45</u>	82.01	78.86	75.52	70.18
pixelate	61.24	90.03	<u>88.61</u>	85.99	83.06	79.5	73.84
jpeg compression	65.8	90.47	<u>88.54</u>	86.0	82.89	79.44	73.9
speckle noise	40.73	86.91	<u>86.75</u>	84.58	81.57	78.27	73.12
gaussian blur	55.78	83.45	<u>82.4</u>	80.8	77.91	74.88	69.7
spatter	75.03	88.26	<u>86.76</u>	84.12	81.11	77.79	72.64
saturate	81.47	90.04	<u>87.96</u>	85.07	82.02	78.65	73.28
Avg.	58.48	84.0	<u>82.49</u>	79.74	76.68	73.53	68.48

Table 21: Accuracy of ϵ -robust WideResNet-18 models ($\epsilon = 2, 4, 6, 8, 10, 12$) on various common corruptions. The bold and underlined values denote the largest and second largest value in each row (*i.e.*, for each type of corruption).